



**Covariant description of contact interfaces
considering anisotropy for adhesion and friction
Part 1
Formulation and analysis of the computational
model**

Alexander Konyukhov, Karl Schweizerhof
Universität Karlsruhe, Institut für Mechanik

Institut für Mechanik
Kaiserstr. 12, Geb. 20.30
76128 Karlsruhe
Tel.: +49 (0) 721/ 608-2071
Fax: +49 (0) 721/ 608-7990
E-Mail: ifm@uni-karlsruhe.de
www.ifm.uni-karlsruhe.de

Covariant description of contact interfaces considering anisotropy for adhesion and friction

Part 1.

Formulation and analysis of the computational model.

Alexander Konyukhov, Karl Schweizerhof

2006

Abstract.

A covariant description for contact problems including anisotropy for both adhesion and sliding domains is proposed. The principle of maximum dissipation is used to obtain a computational model in the case of quasi-static motion. Various cases including curvilinear anisotropy on arbitrary surfaces illustrating the possibility to model machined surfaces are considered. The part is served to be a necessary preparation for further finite element implementations and numerical analysis.

Keywords.

covariant description, anisotropy, contact, adhesion, Coulomb friction

1 Introduction

The majority of contact problems is solved under the assumption of smoothness of contact surfaces. However, some cases appear in practice when it is impossible to neglect the roughness of the contact surfaces. Essentially two types can be distinguished: a) when a surface has randomly distributed asperities, and b) when asperities have algorithmic structure, e.g. the surface shows different macro properties in different directions.

Mechanical characteristics for the contact problem of the first type a) are obtained via statistically distributed asperities. Statistical analysis of a real rough surface and experimental aspects of its measurements have been developed in series of publications: Longuet-Higgins [20], Greenwood and Williamson [9], Whitehouse and Archard [30] and more recently Whitehouse and Phillips [31] and Greenwood [10]. A comparative analysis of these surface models is presented in McCool [22].

A statistical concept for the contact in the context of finite element methods was developed then in Zavarise et.al. [37], Wriggers and Zavarise [35], [36] for the non-frictional contact with normally distributed asperities. Buczkowski and Kleiber [5] considered first non-frictional contact with an isotropical statistical distribution of asperities, and then in [6] non-frictional contact with an anisotropic statistical distribution of asperities. The modeling of a contact surface with Bezier splines according to the statistical distribution of asperities was considered in Bandeira, Wriggers and Pimenta [2]. Various nonlinear friction models are considered in the monography of Wriggers [33].

A generalization of the isotropic macro characteristics is used to describe frictional contact problems of the second type b). Michalowski and Mroz [24] considered the sliding of a rigid block on an inclined surface and formulated various sliding rules for sliding displacements

which depend on directions. Thus, an anisotropic friction model for sliding was introduced. In a purely theoretical description Zmitrowicz [38] developed the structure of the friction tensor for sliding forces based on the motion of an elementary block on an anisotropic surface and described its properties based on symmetry groups for the tensor. Curnier [7] presented a rate independent theory of anisotropic friction for contact interaction mentioning adhesion as a possible elastic part without any further development. Zmitrowicz [39] developed the structure of the sliding friction tensor according to a relative sliding velocity and introduced a classification of anisotropic surfaces based on the number of eigenvalues of the friction tensor. These cases were numerically illustrated for a material point on the anisotropic plane. He and Curnier [12] used the theory of tensor function representations to obtain the structure of the friction tensor for an arbitrary nonlinear case according to the relative sliding velocity and derived also thermodynamical restrictions for the friction tensor components. Mroz and Stupkiewicz [24] considered the structure of the friction tensor based on a statical model of interaction of springs located in a plane which has periodically inclined asperities.

Despite the extensive literature on finite element solutions for contact problems, there are only few publications on finite element models for anisotropic friction. Buczkowski and Kleiber [4], [6] created an interface element containing the orthotropic sliding law. The return-mapping scheme in a Cartesian coordinate system was then used to obtain the sliding displacements. The effect of orthotropy was interpreted considering small displacements for a flat punch on an elastic foundation. Hjjaj et. al. [13] formulated the problem via the bi-potential and applied Lagrangian multiplier methods to solve a problem with orthotropic friction considering also small displacements in Cartesian coordinates. Parametric quadratic programming was used in Zhang et. al. [42] to solve the almost identical problem. Recently, Jones and Papadopoulos [26] developed a finite element model for anisotropic friction, where the stick-slip condition is enforced via Lagrange multipliers.

The aforementioned publications include anisotropy only for the friction model and **do not assume any anisotropy for the elastic region, the adhesion**. In the current contribution we propose a general approach for the finite element solution of quasi-static frictional contact problems including anisotropy for both adhesion and sliding assuming that contact surfaces in general possess an anisotropic structure for both, elastic and friction domains. This approach is based on the covariant description for contact problems which is applicable for an arbitrary geometry of contact surfaces and large displacements. Within the covariant description, as given in Konyukhov and Schweizerhof [14], [15] contact conditions are described on the tangent plane of the contact surface exploiting tensor analysis. Using a penalty regularization of Coulomb's friction law and the return-mapping algorithm leads to the evolution equations for contact friction. It becomes obvious, that the evolution equations are not only a regularization technique, but act also as the constitutive relation to model friction behavior for an adhesion domain. Keeping this idea in mind, the evolution equations are generalized for a more complex mechanical behavior exploiting tensor algebra on the tangent plane of the contact surface. The covariant description allows to formulate the main characteristics for surfaces with arbitrary geometry, e.g. the yield function is formulated via the friction tensor defined in surface metrics. Then both, anisotropy for adhesion resp. sticking and anisotropy for sliding are treated. Anisotropic resp. orthotropic tensors inherit their properties either from the spectral decomposition or, in the more general case, from arbitrary curvilinear coordinate systems defined on the surface. The last case has advantages in practical applications as e.g. for a homogenized average model of machined surfaces. This structure of tensors automatically satisfies all necessary theoretical restrictions developed earlier in [12] and [39]. Thus, a consistent model for anisotropic surfaces can be developed.

In order to define sliding forces as well as sliding displacements the principle of maximum dissipation is used. All models allow representative geometrical interpretations on the tangent plane. Via this principle, the sliding forces and sliding displacements are derived in the covariant form. The formulation in the covariant form easily allows to derive the consistently linearized equations, which are necessary for the iterative solution within a Newton type scheme, even for the case with nonlinear anisotropy in the reference Cartesian coordinate system.

The article is subdivided into two parts, where the current part is organized as follows: In the second section we recall all necessary details from the covariant description for the isotropic case. The generalization for the adhesive part and for the sliding part for the arbitrary geometry is developed in section 3. The orthotropic planar cases in Cartesian as well as in polar coordinates are considered as particular structures of tensors. As a specific case with curvilinear geometry spiral orthotropy for a cylinder is considered. The fourth section deals with the formulation of the friction problem as maximization problem for the energy dissipation function. Here also the geometrical interpretation of the derived model is discussed. The consistent linearization on the tangent plane, the finite element implementation and a discussion about the robustness of the developed approach on the basis of various numerical examples are included in the second part.

2 Basis of the covariant description

Several computational approaches for isotropic Coulomb frictional contact in context with finite element analysis have been developed in the literature. The general models – all using the elastoplastic analogy and the return-mapping algorithm for the penalty regularization of the friction law – are developed in Wriggers et. al. [32], Laursen and Simo [18], Peric and Owen [28], Parisch and Lübbing [27]. Reviews of contemporary contact models can be found in the monographs of Wriggers [33] and Laursen [19]. The covariant description was especially developed in Konyukhov and Schweizerhof [14], [15] to take advantage of the differential properties of contact surfaces. These derivations allow a straightforward geometrical interpretation of the characteristics for an iterative solution, such as regularization equations and tangent matrices. In the current section all important details of the covariant description necessary for a further generalization into the anisotropic domain are briefly outlined.

As starting basis of the covariant description, we introduce a spatial local coordinate system related to the master surface. This coordinate system is defined fitting the closest projection procedure. Let \mathbf{S} be a slave point and \mathbf{C} its projection on the surface, see Fig. 1. At point \mathbf{C} we consider a coordinate system based on the following relation:

$$\mathbf{r}_s(\xi^1, \xi^2, \xi^3) = \boldsymbol{\rho}(\xi^1, \xi^2) + \mathbf{n}\xi^3. \quad (1)$$

The first two convective coordinates ξ^1, ξ^2 define properties of the surface and, therefore, are responsible for the tangential contact interaction. The third coordinate ξ^3 is the value of the penetration and is used to define the properties of the normal interaction. It is obtained after the aforementioned closest point procedure as projection on the third axis \mathbf{n} in each iteration step:

$$\xi^3 = (\mathbf{r}_s - \boldsymbol{\rho}) \cdot \mathbf{n}. \quad (2)$$

The basis vectors \mathbf{r}_i , $i = 1, 2, 3$ of the spatial coordinate system eqn. (1) are obtained via

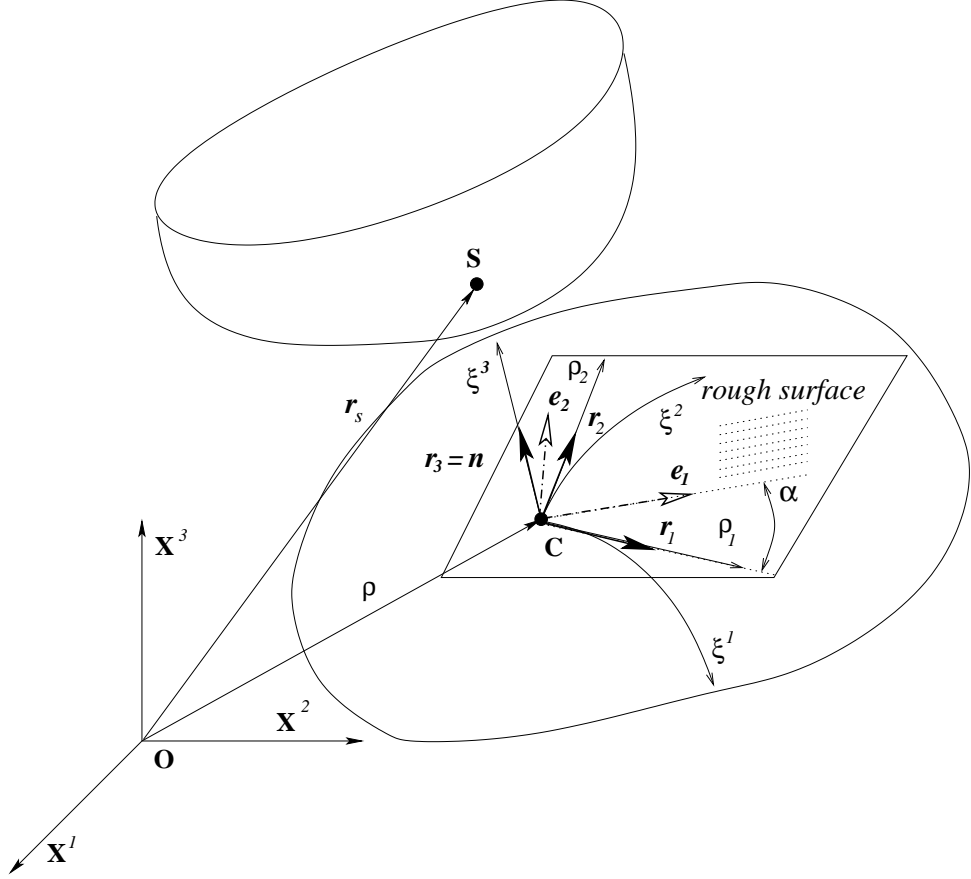


Figure 1: Contact between bodies. Definitions for closest point projection. Anisotropic contact surface.

the basis surface vectors $\rho_1, \rho_2, \mathbf{n}$ as:

$$\mathbf{r}_i = \frac{\partial \mathbf{r}}{\partial \xi^i} = \rho_i + \mathbf{n}_i \xi^3 = (a_i^k - h_i^k \xi^3) \rho_k, \quad i, k = 1, 2, \quad \mathbf{r}_3 = \mathbf{n}, \quad (3)$$

where a_i^k are mixed components of the surface metric tensor and h_i^k are mixed components of the surface curvature tensor. A core of the covariant description is to consider contact dependencies in the 3D spatial system and to express them on the tangent plane, i.e. at $\xi^3 = 0$.

2.1 Convective velocities. Variation of relative displacements.

Projections of the full time derivative of eqn. (1) to the local basis \mathbf{r}_i considered at $\xi^3 = 0$ result in the convective velocities $\dot{\xi}^i$. The tangential components are defined as

$$\dot{\xi}^j = a^{ij} (\mathbf{v}_s - \mathbf{v}) \cdot \rho_i, \quad i, j = 1, 2, \quad (4)$$

where \mathbf{v}_s is the velocity of the slave point S , and \mathbf{v} is the velocity of the projection point C . The third component is given by the value in the normal direction

$$\dot{\xi}^3 = (\mathbf{v}_s - \mathbf{v}) \cdot \mathbf{n}, \quad i = 1, 2. \quad (5)$$

Considering the convective velocities also the variation of the relative displacements can be expressed in form of $\delta \xi^i$

$$\delta \mathbf{r}_s - \delta \rho = \delta \xi^i \rho_i + \delta \xi^3 \mathbf{n}. \quad (6)$$

2.2 Evolution equations for contact tractions

The vector of contact tractions \mathbf{R} is defined as a covariant vector and, therefore, is expressed via the contravariant basis vectors $\boldsymbol{\rho}^i$ and \mathbf{n} as sum of the tangential and normal components

$$\mathbf{R} = \mathbf{T} + \mathbf{N} = T_i \boldsymbol{\rho}^i + N \mathbf{n}. \quad (7)$$

As is well known, the relations between two coordinates ξ^1, ξ^2 and the tangential force can be formulated in the differential form as so-called evolution equations. The penalty regularization process for the simple Coulomb friction law within the analogy to the rigid plasticity model leads to the following evolution equations for the trial tangential contact tractions T_i :

$$\frac{dT_i}{dt} = (-\epsilon_T a_{ij} + \Gamma_{ij}^k T_k) \dot{\xi}^j - h_i^k T_k \dot{\xi}^3, \quad (8)$$

where Γ_{ij}^k are the Christoffel symbols for the contact surface. Eqn. (8) serves to compute the trial tangent tractions. The final values are obtained via the return-mapping scheme, see [19], [33]. Equation (8) is a covariant scalar form of the proportionality condition between the full time derivative of the tangent traction vector \mathbf{T} and the relative velocity vector $\dot{\xi}^i \boldsymbol{\rho}_i$ expressed on the tangent plane

$$\frac{d\mathbf{T}}{dt} = -\epsilon_T \dot{\xi}^i \boldsymbol{\rho}_i, \quad (9)$$

where a full time derivative $\frac{d\mathbf{T}}{dt}$ is taken in covariant form

$$\frac{d\mathbf{T}}{dt} = \frac{DT_i}{dt} \boldsymbol{\rho}^i, \quad \frac{DT_i}{dt} \equiv \frac{dT_i}{dt} - \Gamma_{ij}^k T_k \dot{\xi}^j + h_i^k T_k \dot{\xi}^3, \quad (10)$$

The regularization equation for the normal traction N satisfying the non-penetrability condition has the following form:

$$N = \epsilon_N H(-\xi^3) \xi^3, \quad (11)$$

where a Heaviside function $H(-\xi^3)$ reflects the fact that N is not equal zero and is computed only when a penetration occurs, i.e. $\xi^3 < 0$.

The full time derivative \dot{N} is then:

$$\dot{N} = -\epsilon_N H(-\xi^3) \dot{\xi}^3. \quad (12)$$

2.2.1 Integration of evolution equations. Geometrical interpretation of the return-mapping scheme.

As shown in Konyukhov and Schweizerhof [14], [15], within the contact description the curvature part can be omitted in numerous cases without loss of efficiency leading to considerable simplifications and a major gain in numerical effort. This is especially pronounced for such contact problems, where the development of sticking-sliding zones is important. In such cases we can e.g. simplify all equations, assuming constant metrics. The evolution equation is solved then numerically via the implicit backward scheme with n indicating the load step arising from a subdivision of the loads applied in sequential load steps.

$$T_i^{(n+1)} = T_i^{(n)} - \epsilon_T a_{ij} (\xi_{(n+1)}^j - \xi_{(n)}^j) = \quad (13)$$

continuing recursively:

$$= T_i^{(n-1)} - \epsilon_T a_{ij} (\xi_{(n)}^j - \xi_{(n-1)}^j) - \epsilon_T a_{ij} (\xi_{(n+1)}^j - \xi_{(n)}^j)$$

$$\begin{aligned}
&= T_i^{(n-1)} - \epsilon_T a_{ij} (\xi_{(n+1)}^j - \xi_{(n-1)}^j) = \dots \\
&= T_i^{(0)} - \epsilon_T a_{ij} (\xi_{(n+1)}^j - \xi_{(0)}^j)
\end{aligned}$$

Assuming that the initial tangential forces are zero, $T_i^{(0)} = 0$, we get

$$T_i^{(n+1)} = -\epsilon_T a_{ij} \Delta \xi^j, \quad \text{with } \Delta \xi^j = (\xi_{(n+1)}^j - \xi_{(0)}^j). \quad (14)$$

Eqn. (14) defines trial tractions T_i at load step $(n+1)$ at contact points on the tangent plane $\xi_{(n+1)}^1, \xi_{(n+1)}^2$. The absolute value of the tangent traction is computed as:

$$\|\mathbf{T}\|^2 = T_i^{(n+1)} T_j^{(n+1)} a^{ij} = \epsilon_T^2 a_{ij} (\xi_{(n+1)}^i - \xi_{(0)}^i) (\xi_{(n+1)}^j - \xi_{(0)}^j). \quad (15)$$

With eqn. (15) the sticking zone in combination with the Coulomb law becomes then:

$$\|\mathbf{T}\|^2 \leq \mu |N|^2 \implies \epsilon_T^2 a_{ij} (\xi_{(n+1)}^i - \xi_{(0)}^i) (\xi_{(n+1)}^j - \xi_{(0)}^j) \leq \mu^2 N^2. \quad (16)$$

Eqn. (16) describes a circle in a Cartesian coordinate system via the convective coordinates ξ_1, ξ_2 . The circle is placed on the tangent plane with the center at $\xi_{(0)}^1, \xi_{(0)}^2$. The inner part of it defines the allowable elastic region for the projection of a slave point, the so-called adhesion domain. Thus, the geometrical interpretation of the solution of the evolution equation is a trajectory of the contact point which is allowed to be inside the circle in the case of sticking. If eqn. (11) is taken for regularization of the normal traction N , then we obtain a cone equation in the spatial coordinate system:

$$\epsilon_T^2 a_{ij} (\xi_{(n+1)}^i - \xi_{(0)}^i) (\xi_{(n+1)}^j - \xi_{(0)}^j) \leq \mu^2 \epsilon_N^2 (\xi^3)^2. \quad (17)$$

This interpretation can be found in Krstolovic-Opara and Wriggers [17], where a so-called "frictional cone description" was proposed.

2.3 Weak form.

The work of the contact tractions \mathbf{R} in eqn. (7) on the relative virtual displacement $\delta \mathbf{r}_s - \delta \boldsymbol{\rho}$ in eqn. (6) can be expressed on the contact surface as:

$$\delta W_c = \int_s \mathbf{R} \cdot (\delta \mathbf{r}_s - \delta \boldsymbol{\rho}) ds = \int_s N \delta \xi^3 ds + \int_s T_j \delta \xi^j ds. \quad (18)$$

The integral in eqn. (18) is computed on the slave surface ds , whereas all functions are defined on the master surface.

3 Generalization for complex contact interface laws

The regularization for a Coulomb type frictional law leads to a subdivision of the motion of the contact point on the master surface into reversible and irreversible parts. The first, reversible part appears due to the regularization and usually contains a penalty parameter. It describes the elastic tangent deformation, the so-called tangential adhesion, see Curnier [7]. The second, irreversible part is described by a flow rule due to a specific yield function. Both parts can be generalized for anisotropic domains by taking proper tensors and equations. In this section, we summarize all necessary equations in vector form convenient for the expansion

into the anisotropic domain. For the representations of the anisotropic tensor we will use the representation based on the spectral decomposition in the simple case of constant orthotropy, and in the general case, the representation based on the tensor product of unit vectors of an arbitrary curvilinear surface coordinate system.

3.1 Vector form of the isotropic equations

The generalization is based upon the consideration of anisotropic tensors instead of isotropic tensors in the evolution equations. The structure of the anisotropic tensors for contact, if one or both contact surfaces have anisotropic structure is theoretically discussed by Zmitrowicz [38], [39] and also by He and Curnier [12]. Here we assume the described properties for tensors and will further discuss some restrictions for both the adhesion tensor and the friction tensor. All tensors are defined in the basis of the tangent plane of the contact master surface.

3.1.1 Elastic part of the contact deformation

To start the development, we reorganize the evolution equations (8) and (12), describing in fact the elastic reversible part of the deformation in vector form in the local surface coordinate system.

$$\frac{d\mathbf{R}}{dt} = \hat{\mathbf{E}}\mathbf{v}^r, \quad (19)$$

where \mathbf{R} is a traction vector acting on a slave point S ; $\mathbf{v}^r = \mathbf{v}_s - \mathbf{v} = \boldsymbol{\rho}_i \dot{\xi}^i + \mathbf{n} \dot{\xi}^3$ is a relative velocity of a slave point and $\hat{\mathbf{E}}$ is an isotropic tensor of penalty parameters:

$$\hat{\mathbf{E}} = \begin{bmatrix} -\epsilon_T & 0 & 0 \\ 0 & -\epsilon_T & 0 \\ 0 & 0 & -\epsilon_N \end{bmatrix}. \quad (20)$$

Eqn. (19) describes the force-displacement relationship in a rate form for the reversible elastic part of the contact interaction. The irreversible part in the case of a simple Coulomb friction law is correlated to the rigid plasticity model.

3.1.2 Yield function for the isotropic Coulomb friction law

Remembering, that the scalar product is computed on the surface via the metric tensor components a^{ij} , we can define a yield function for the Coulomb friction law as

$$\Phi := \frac{\sqrt{\mathbf{T} \cdot \mathbf{T}}}{\mu|N|} - 1 \equiv \frac{\sqrt{T_i T_j a^{ij}}}{\mu|N|} - 1. \quad (21)$$

The sticking and sliding zones are now defined by the rule:

$$\Phi \leq 0 \text{ means } \textit{sticking}; \quad \Phi > 0 \text{ means } \textit{sliding}. \quad (22)$$

Irreversible parts including the sliding forces etc. can be obtained via the flow rule.

3.2 General interface model

In order to take into account a diversity of linear mechanical models including viscoelasticity etc., we can generalize eqn. (19) as follows:

$$\frac{d\mathbf{R}}{dt} + \hat{\mathbf{A}}\mathbf{R} = \hat{\mathbf{B}}\mathbf{v}^r + \hat{\mathbf{C}}\Delta\xi, \quad (23)$$

where $\hat{\mathbf{A}}, \hat{\mathbf{B}}, \hat{\mathbf{C}}$ are tensors defined in the local surface coordinate system and $\Delta\xi$ is a vector of the relative displacements

$$\Delta\xi = \Delta\xi^i \boldsymbol{\rho}_i + \Delta\xi^3 \mathbf{n}, \quad \Delta\xi^i = \xi^i - \xi_{(0)}^i, \quad i = 1, 2, 3. \quad (24)$$

A point with convective coordinates $\xi_{(0)}^i$ indicates an initial position where the contact traction vector \mathbf{R} equals zero, i.e.

$$\mathbf{R}|_{\xi^i = \xi_{(0)}^i} = \mathbf{0}. \quad (25)$$

The equation for the elastic region in the form of eqn. (23) covers various viscoelastic models such as Maxwell and Kelvin models in arbitrary anisotropic forms including adhesion. A generalization of the isotropic Coulomb friction model according to Maxwell and Kelvin viscoelastic models was considered in Araki and Hjelmstad [1]. A rate-dependent model with orthotropic friction coefficients in Cartesian coordinate system was considered in Oancea and Laursen [25].

Assuming the decoupling of the third normal coordinate ξ^3 , we can rewrite eqn. (23) for the surface components in the form:

$$\frac{d\mathbf{T}}{dt} + \mathbf{A}\mathbf{T} = \mathbf{B}\mathbf{v}^r + \mathbf{C}\Delta\xi, \quad (26)$$

where $\mathbf{A}, \mathbf{B}, \mathbf{C}$ are tensors defined on the tangent plane, \mathbf{T} is a tangent force vector, $\mathbf{v}^r = \mathbf{v}_s - \mathbf{v}$ is a relative tangent velocity vector expressed on the tangent plane, $\Delta\xi = \Delta\xi^i \boldsymbol{\rho}^i$ is a relative tangent displacement vector and $\frac{d}{dt}$ is a full time derivative in the covariant form on the contact surface.

The third equation for the normal force N and for the penetration ξ^3 , is treated separately

$$\dot{N} + aN = b\dot{\xi}^3 + c\Delta\xi^3. \quad (27)$$

For the further development we consider only a rate independent motion, i.e. assume a specific structure of the evolution equations (23) and (27) excluding the direct time dependency of the contact tractions.

3.2.1 Anisotropic evolution equations. Rate-independent model.

Considering a case of rate-independent motions by taking $\mathbf{A} = \mathbf{0}, \mathbf{C} = \mathbf{0}$ in eqn. (26) and $a = 0, c = 0$ in eqn. (27) we define anisotropy for an elastic part of the contact conditions. Therefore, from eqn. (26) the following rate forms remain:

$$\frac{d\mathbf{T}}{dt} = \mathbf{B}(\mathbf{v}_s - \mathbf{v}). \quad (28)$$

Expressing this in the tangent plane by coordinates, we get the following evolution equation

$$\frac{\partial T_i}{\partial t} + \nabla_j T_i \dot{\xi}^j = b_{ij} \dot{\xi}^j, \quad j = 1, 2. \quad (29)$$

The evolution equations (28) resp. (29) describe the fact that the reaction tangential forces are acting not in the opposite direction to the velocity vector, but in the direction defined by tensor \mathbf{B} . In other words, if a force \mathbf{T} is acting on point C on the surface, then this point is moved in a somewhat different direction defined by the angle β , see Fig. 2, but, in general, not in the direction of the force.

Remark. The evolution equations (28) describe the elastic deformations of contact interaction in the rate form. This elastic tangential deformation is known as tangential adhesion, see Curnier [7]. Thus, we call a tensor \mathbf{B} **the elastic adhesion tensor**, or simply **the adhesion tensor**.

Remark. The mechanical restriction for the elastic force \mathbf{T} to act in opposite direction to the relative velocity can be formulated in an energy sense according to the thermodynamical restriction: the power of the elastic force \mathbf{T} must be negative. This requires that **the adhesion tensor taken with a minus sign $-\mathbf{B}$** is a positively defined tensor.

Since we are working with a decoupled model regarding the normal and tangential contact interactions, the evolution equation for the normal force N and thus the parameter b in eqn. (27) is kept in the form given by eqn. (12).

3.3 Anisotropic yield function

Several theoretical approaches are known in literature for formulations for the yield function and for the sliding rule. Before presenting a particular structure of the tensor we will briefly review these approaches as well as restrictions for the tensor which are known in literature.

3.3.1 Various approaches for formulations of yield criteria and sliding rules

In a first publication, Michalowski and Mroz [23] proposed to distinguish functions for limit criteria and for sliding, introducing the so-called associated and non-associated sliding rules. These functions were built by analogy looking at the solution for the sliding of a rigid block on an inclined surface.

Zmitrowicz [38] introduced the friction tensor \mathbf{F} into the originally isotropic Coulomb criteria (21) and described its properties based on the groups of material symmetry. The sliding forces were formulated directly without correspondence to the yield criteria. It was also obtained that *"There is no restrictions for the arbitrary anisotropic friction tensor except its positive definition, but the orthotropic friction tensor is symmetric"*. The superposition of two friction tensors when two anisotropic surfaces are in contact was also discussed. In a later publication Zmitrowicz [39] assumed that the sliding force nonlinearly depends on the relative velocity introducing in addition a 4th-order friction tensor.

He and Curnier [12] applied the theory of tensor function representations – the fundamental aspects of this theory see Zheng [43] – to obtain the general irreducible structure for the nonlinear friction tensor in the case of friction between two orthotropic surfaces. The structure at the contact point is defined by [12] as follows:

- \mathbf{m} is a unit vector of the preferable direction for the first surface,
- \mathbf{k} is a unit vector of the preferable direction for the second surface,
- \mathbf{u} is a unit vector of the relative sliding velocity.

Then the sliding force \mathbf{T} is defined as

$$\mathbf{T} = N [\alpha_1(I_1, I_2)\mathbf{E} + \alpha_2(I_1, I_2)(\mathbf{m} \otimes \mathbf{m}) + \alpha_3(I_1, I_2)(\mathbf{k} \otimes \mathbf{k})] \mathbf{u}, \quad (30)$$

where N is a normal force, \mathbf{E} is a unit tensor, α_i are scalar functions of the following invariants: $I_1 = \mathbf{u} \cdot (\mathbf{m} \otimes \mathbf{m})\mathbf{u}$, $I_2 = \mathbf{u} \cdot (\mathbf{k} \otimes \mathbf{k})\mathbf{u}$. Also the symmetric properties of the friction tensor for orthotropic surfaces were derived and it was shown, that a yield function is a direct consequence of the rate-independence condition. Other important results were "*the thermodynamical restrictions for the friction tensor leading to its positivity and the formulation of the convex energy dissipation function*".

3.3.2 Coulomb type yield functions

Summarizing the results of the previous developments, we will later use a generalization of the isotropic yield criterion in eqn. (21) by replacing the scaled metric components $a^{ij}/\mu^2 N^2$ with tensor components f^{ij} , assuming the a-priori necessary properties as discussed above. Thus, we can obtain:

$$\Phi_N = \sqrt{f_N^{ij} T_i T_j} - 1 = \sqrt{(\mathbf{T} \cdot \mathbf{F}_N \mathbf{T})} - 1. \quad (31)$$

The standard assumption of *proportionality of the sliding force \mathbf{T}^{sl} to the normal traction N* , the so-called Coulomb's form, see Curnier [7], leads to

$$\mathbf{F}_N = \frac{\mathbf{F}}{N^2}, \quad (32)$$

and the yield function can then be written as:

$$\Phi = \sqrt{f^{ij} T_i T_j} - |N| = \sqrt{\mathbf{T} \cdot \mathbf{F} \mathbf{T}} - |N|. \quad (33)$$

The sliding criteria (21-22) become then

$$\text{if } \Phi \leq 0 \text{ then } \textit{sticking}, \quad (34)$$

describing a contact point inside the adhesion domain,

$$\text{if } \Phi > 0 \text{ then } \textit{sliding}, \quad (35)$$

describing a contact point outside the adhesion domain.

The tensor \mathbf{F} is called **friction tensor** and is defined by its components f^{ij} in the surface tensor basis as

$$\mathbf{F} = f^{ij} \boldsymbol{\rho}_i \otimes \boldsymbol{\rho}_j. \quad (36)$$

Comparing with the isotropic function, we introduce anisotropic friction coefficients:

$$f^{ij} = \frac{a^{ij}}{\mu_{ij}^2}, \quad i, j = 1, 2, \quad (37)$$

where μ_{ij} are coefficients of friction.

3.4 Tensor representations for anisotropy

Here we consider particular structures for the anisotropic tensors for the evolution equations (28) as well as for the yield function (33), automatically satisfying the necessary restrictions mentioned in the previous sections. We start with the simplest case – a constant orthotropy on the plane. In this case all tensors are symmetrical ones. The more general anisotropic case can be defined then in an arbitrary coordinate system by setting different properties along the coordinate lines.

3.4.1 Spectral representation of the tensor – constant orthotropy in the plane.

As mentioned above, constant orthotropy in the plane is described by constant symmetric tensors for which a spectral representation is chosen. Any symmetric positive tensor \mathbf{A} can be decomposed as:

$$\mathbf{A} = \mathbf{Q}\mathbf{\Lambda}\mathbf{Q}^T, \quad (38)$$

where $\mathbf{\Lambda}$ is defined in the mixed tensorial basis as a diagonal matrix of eigenvalues:

$$\mathbf{\Lambda} = \begin{bmatrix} \lambda_1 & 0 \\ 0 & \lambda_2 \end{bmatrix}; \quad (39)$$

and \mathbf{Q} is an orthogonal tensor. Since it describes the rotation on the tangent plane between the main axes \mathbf{e}_i and the axes ξ^i , see Fig. 2, it becomes

$$\mathbf{Q}_\alpha = \begin{bmatrix} \cos \alpha & -\sin \alpha \\ \sin \alpha & \cos \alpha \end{bmatrix}. \quad (40)$$

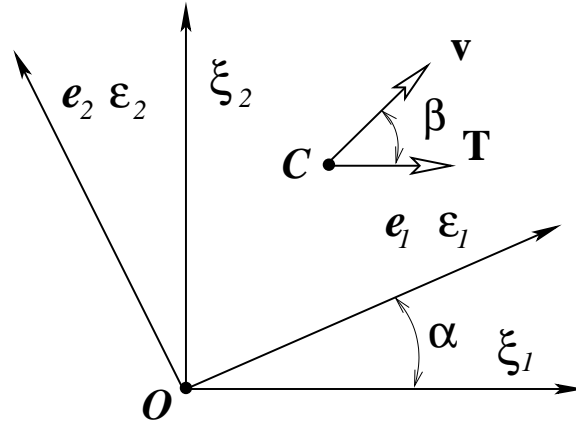


Figure 2: Main orthotropy axes and local surface coordinate system.

The main axes are hereby defined as orthotropy axes. Then the spectral representation of \mathbf{A} is obtained as

$$\mathbf{A} = \mathbf{Q}_\alpha \mathbf{\Lambda} \mathbf{Q}_\alpha^T = [A_j^i] = \begin{bmatrix} \lambda_1 \cos^2 \alpha + \lambda_2 \sin^2 \alpha & (\lambda_1 - \lambda_2) \sin \alpha \cos \alpha \\ (\lambda_1 - \lambda_2) \sin \alpha \cos \alpha & \lambda_1 \sin^2 \alpha + \lambda_2 \cos^2 \alpha \end{bmatrix}. \quad (41)$$

Taking into account, that the model for constant orthotropic friction contains the tensor in the evolution equations (28) and in the yield function (33) in mixed form which allows the spectral decomposition given in eqn. (41), the following derivations are possible:

First we focus on **the evolution equation** given by eqn. (29), where the mixed components are introduced via the spectral decomposition (41). Taking into account that the adhesion tensor \mathbf{B} (see Remark 3.2.1 in Sec. 3.2.1) is negative, we introduce positive values $\varepsilon_i = -\lambda_i > 0$ and an orthotropy angle α . Thus, after a transformation into a local coordinate system the following matrix description for the tensor is obtained:

$$\mathbf{B} = [b_j^i] = - \begin{bmatrix} \varepsilon_1 \cos^2 \alpha + \varepsilon_2 \sin^2 \alpha & (\varepsilon_1 - \varepsilon_2) \sin \alpha \cos \alpha \\ (\varepsilon_1 - \varepsilon_2) \sin \alpha \cos \alpha & \varepsilon_1 \sin^2 \alpha + \varepsilon_2 \cos^2 \alpha \end{bmatrix}. \quad (42)$$

Matrix \mathbf{B} in eqn. (42) describes the orthotropic properties in the reversible part of the tangential interaction, where the parameters $\varepsilon_1, \varepsilon_2$ can be seen as orthotropic moduli of the tangential adhesion. Assuming $\varepsilon_1 = \varepsilon_2$ leads to isotropic behavior and then the isotropic evolution equation is recovered.

Second, **the yield function** for the constant orthotropic friction is defined via the orthotropic friction tensor \mathbf{F} which allows a spectral decomposition. After introducing the angle β between the local coordinate axes and the orthotropy axes, and eigenvalues as $\lambda_i = 1/\mu_i^2$, the following matrix $[f_k^i]$ is obtained:

$$\mathbf{F} = [f_k^i] = \begin{bmatrix} \frac{1}{\mu_1^2} \cos^2 \beta + \frac{1}{\mu_2^2} \sin^2 \beta & (\frac{1}{\mu_1^2} - \frac{1}{\mu_2^2}) \sin \beta \cos \beta \\ (\frac{1}{\mu_1^2} - \frac{1}{\mu_2^2}) \sin \beta \cos \beta & \frac{1}{\mu_1^2} \sin^2 \beta + \frac{1}{\mu_2^2} \cos^2 \beta \end{bmatrix}. \quad (43)$$

The restriction of positivity for the friction tensor \mathbf{F} leads to the known positive orthotropic friction coefficients $\mu_i > 0$.

3.4.2 Structure of the anisotropic tensor inherited from an arbitrary surface curvilinear coordinate system

We assume that on the surface defined via the Gaussian coordinates ξ^1, ξ^2 as

$$\boldsymbol{\rho} = \boldsymbol{\rho}(\xi^1, \xi^2), \quad \boldsymbol{\rho} = \left\{ \begin{array}{l} x_1(\xi^1, \xi^2) \\ x_2(\xi^1, \xi^2) \\ x_3(\xi^1, \xi^2) \end{array} \right\} \quad (44)$$

another Gaussian coordinate system is defined. Thus, the Cartesian coordinates of the same surface x_i are defined by Gaussian convective coordinates α^1, α^2 :

$$x_i = \phi_i(\alpha^1, \alpha^2), \quad i = 1, 2, 3. \quad (45)$$

One can say, that we have re-parameterization of the surface

$$\alpha^i = \alpha^i(\xi^1, \xi^2), \quad i = 1, 2, \quad (46)$$

or, in another words, eqn. (46) defines a new coordinate system on the same surface.

Arbitrary anisotropic properties of a surface can be defined as different characteristics along these coordinate lines. The unit tangent vectors along the coordinate lines are then defined as:

$$\mathbf{e}_i = \frac{\mathbf{r}_i}{\sqrt{g_{ii}}}, \quad i = 1, 2 \quad \text{no summation over } i \quad (47)$$

where $\mathbf{r}_i = \frac{\partial \mathbf{r}}{\partial \alpha_i}$ are the basis vectors, and $g_{ii} = \mathbf{r}_i \cdot \mathbf{r}_i$ are diagonal coefficients of the covariant metrics tensor.

The tensor of anisotropy \mathbf{A} can then be defined via the unit tensor basis as:

$$\mathbf{A} := \lambda_1 \mathbf{e}_1 \otimes \mathbf{e}_1 + \lambda_2 \mathbf{e}_2 \otimes \mathbf{e}_2 = \lambda_1 \frac{\mathbf{r}_1 \otimes \mathbf{r}_1}{g_{11}} + \lambda_2 \frac{\mathbf{r}_2 \otimes \mathbf{r}_2}{g_{22}} = \lambda_i \frac{\mathbf{r}_i \otimes \mathbf{r}_i}{g_{ii}}. \quad (48)$$

Remark. From now on and further in the last representation in eqn. (48) the summation convention is implied also for the sum over i -index, though the index i is repeated four times.

It is obvious, that the tensor structure prescribed above, see eqn. (30), is preserved. As a next step a transformation into the surface basis $\boldsymbol{\rho}_i(\xi^1, \xi^2)$ is necessary for the evolution equation as well as for the yield equation.

Remark. The tensor in eqn. (48) is defined, in general, via the coordinates α^1, α^2 . We introduce a notation \mathbf{A}^C , if the tensor \mathbf{A} is defined in the global reference Cartesian coordinates, and will keep the notation \mathbf{A} if the tensor is defined after the tensor transformation to the surface coordinate system ξ^1, ξ^2 , eqn. (44).

The evolution equation is transformed as follows. Assuming the stiffnesses along the coordinate lines as $\lambda_i = -\epsilon_i$, we obtain

$$\mathbf{B}^C := - \left(\epsilon_1 \frac{\mathbf{r}_1 \otimes \mathbf{r}_1}{g_{11}} + \epsilon_2 \frac{\mathbf{r}_2 \otimes \mathbf{r}_2}{g_{22}} \right). \quad (49)$$

The tensor \mathbf{B}^C is a Cartesian tensor. Some steps are necessary to transform it to surface coordinates ξ^1, ξ^2 . Substitution into the right hand side of the evolution equation (28) leads to:

$$\mathbf{B}^C(\mathbf{v}_s - \mathbf{v}) := -\epsilon_i \frac{\mathbf{r}_i \otimes \mathbf{r}_i}{g_{ii}} \cdot \boldsymbol{\rho}_j \dot{\xi}^j = -\frac{\epsilon_i (\mathbf{r}_i \cdot \boldsymbol{\rho}_j) \dot{\xi}^j}{g_{ii}} \mathbf{r}_i. \quad (50)$$

The dot product of the evolution equation (28) with $\boldsymbol{\rho}_k$, taking into account eqn. (50), leads to the equation in components according to the surface metrics:

$$\frac{dT_k}{dt} = -\frac{\epsilon_i (\mathbf{r}_i \cdot \boldsymbol{\rho}_k) (\mathbf{r}_i \cdot \boldsymbol{\rho}_j) \dot{\xi}^j}{g_{ii}}. \quad (51)$$

For the further implementation into a finite element code, it is more appropriate to introduce a tensor decomposition:

$$\frac{dT_k}{dt} = -\frac{\epsilon_i \mathbf{r}_i \otimes \mathbf{r}_i}{g_{ii}} : (\boldsymbol{\rho}_k \otimes \boldsymbol{\rho}_j) \dot{\xi}^j, \quad (52)$$

where the components of the first tensor $\mathbf{B}^C = -\frac{\epsilon_i \mathbf{r}_i \otimes \mathbf{r}_i}{g_{ii}}$ can be computed in a Cartesian coordinate system separately for the surface as:

$$b_{ln}^C = -\frac{\epsilon_i}{g_{ii}} \frac{\partial \phi_l}{\partial \alpha_i} \frac{\partial \phi_n}{\partial \alpha_i}. \quad (53)$$

After this the evolution eqn. (52) is defined as:

$$\frac{dT_k}{dt} = b_{ln}^C \frac{\partial x_l}{\partial \xi^k} \frac{\partial x_n}{\partial \xi^j} \dot{\xi}^j. \quad (54)$$

From the last equation the covariant components of the tensor \mathbf{B} in the global surface basis $\boldsymbol{\rho}_1, \boldsymbol{\rho}_2$ are obtained as tensor transformations, i.e.

$$b_{ij} = b_{ln}^C \frac{\partial x_l}{\partial \xi^i} \frac{\partial x_n}{\partial \xi^j}. \quad (55)$$

Introducing the friction coefficients $\lambda_i = 1/\mu_i^2$ into the yield function and then applying analogous tensor operations as for the evolution equation lead to the following form:

$$\Phi = \sqrt{\frac{\mathbf{r}_i \otimes \mathbf{r}_i}{\mu_i^2 g_{ii}} : (T_k T_l \boldsymbol{\rho}^k \otimes \boldsymbol{\rho}^l) - |N|}, \quad (56)$$

from which a similar definition of covariant components for the friction tensor are obtained:

$$f_{kl} = \frac{\mathbf{r}_i \otimes \mathbf{r}_i}{\mu_i^2 g_{ii}} : (\boldsymbol{\rho}^k \otimes \boldsymbol{\rho}^l). \quad (57)$$

In the following we consider particular structures for covariant components in the Cartesian coordinate system b_{ij}^C in eqn. (53) as well as for b_{ij} in eqn. (55) in the local surface coordinate system for the anisotropic plane, for polar orthotropy on a plane and for spiral orthotropy on a cylinder.

3.4.3 Anisotropic plane. Structure of the \mathbf{B}^C and \mathbf{B} tensors in Cartesian coordinates.

On the plane $x_3 = 0$, we consider anisotropic properties defined by two unit vectors \mathbf{r}_1 and \mathbf{r}_2 :

$$\mathbf{r}_1 = \begin{Bmatrix} \cos \alpha \\ \sin \alpha \\ 0 \end{Bmatrix}, \quad \mathbf{r}_2 = \begin{Bmatrix} \cos \beta \\ \sin \beta \\ 0 \end{Bmatrix}. \quad (58)$$

The Cartesian components of the adhesion tensor b_{in}^C are obtained as:

$$\mathbf{B}^C = - \begin{bmatrix} \varepsilon_1 \cos^2 \alpha + \varepsilon_2 \cos^2 \beta & \varepsilon_1 \sin \alpha \cos \alpha + \varepsilon_2 \sin \beta \cos \beta & 0 \\ \varepsilon_1 \sin \alpha \cos \alpha + \varepsilon_2 \sin \beta \cos \beta & \varepsilon_1 \sin^2 \alpha + \varepsilon_2 \sin^2 \beta & 0 \\ 0 & 0 & 0 \end{bmatrix}. \quad (59)$$

For an analysis, the approximation of the surface is necessary in order to obtain the structure of the tensor in surface coordinates ξ^1, ξ^2 in eqn. (55). If the latter coincide with the global Cartesian coordinates $\xi^i = x_i$, we obtain

$$\mathbf{B} = - \begin{bmatrix} \varepsilon_1 \cos^2 \alpha + \varepsilon_2 \cos^2 \beta & \varepsilon_1 \sin \alpha \cos \alpha + \varepsilon_2 \sin \beta \cos \beta \\ \varepsilon_1 \sin \alpha \cos \alpha + \varepsilon_2 \sin \beta \cos \beta & \varepsilon_1 \sin^2 \alpha + \varepsilon_2 \sin^2 \beta \end{bmatrix}. \quad (60)$$

It is obvious, that isotropy is no longer recovered simply by taking $\varepsilon_1 = \varepsilon_2$. However, if we take the unit vectors to be orthogonal, i.e. $\beta = \pi/2 + \alpha$, the orthotropic matrix obtained previously via the spectral representation in eqn. (42) is recovered.

3.4.4 Orthotropic surface in polar coordinates. Structure of the \mathbf{B}^C and \mathbf{B} tensors in Cartesian coordinates.

As an example with curvilinear orthotropy, a plane with orthotropic properties in polar coordinates, see Fig. 3, is considered. These properties are defined by the elastic constants $\varepsilon_r, \varepsilon_\phi$ acting along the coordinate lines. The definition in eqn. (45) is then a transformation to polar coordinates:

$$x = r \cos \phi, \quad y = r \sin \phi, \quad z = 0. \quad (61)$$

The Cartesian components of the orthotropic tensor b_{kn}^C are then defined by the following matrix:

$$\mathbf{B}^C = - \begin{bmatrix} \varepsilon_r \cos^2 \phi + \varepsilon_\phi \sin^2 \phi & (\varepsilon_r - \varepsilon_\phi) \sin \phi \cos \phi & 0 \\ (\varepsilon_r - \varepsilon_\phi) \sin \phi \cos \phi & \varepsilon_r \sin^2 \phi + \varepsilon_\phi \cos^2 \phi & 0 \\ 0 & 0 & 0 \end{bmatrix}. \quad (62)$$

Applying the inverse mapping from polar coordinates to Cartesian coordinates in eqn. (61) (see also eqn. (55)), we obtain:

$$\mathbf{B} = -\frac{1}{x^2 + y^2} \begin{bmatrix} \varepsilon_r x^2 + \varepsilon_\phi y^2 & (\varepsilon_r - \varepsilon_\phi)xy \\ (\varepsilon_r - \varepsilon_\phi)xy & \varepsilon_r y^2 + \varepsilon_\phi x^2 \end{bmatrix}. \quad (63)$$

The adhesion tensor for polar orthotropy in eqn. (63) contains a typical example of nonlinear surface properties in the reference Cartesian coordinate system.

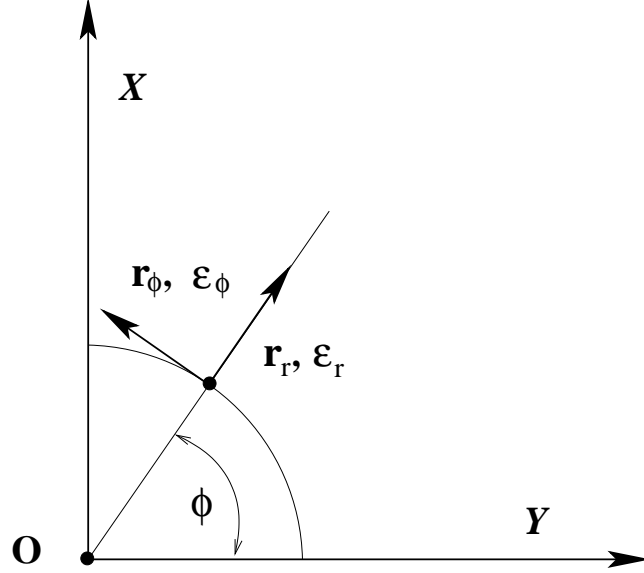


Figure 3: Polar orthotropic surface.

3.4.5 Spiral orthotropy on a cylindrical surface. Structure of the \mathbf{B}^C and \mathbf{B} tensors in cylindrical coordinates.

As a more complex case, we consider a circular cylinder and the surface orthotropy resulting from spiral coordinate lines on the cylinder. This example can be practically interesting to model e.g. screw connections. First, we define a rigid cylinder with a surface described by the following parameterization $\boldsymbol{\rho}(\alpha, z)$:

$$\boldsymbol{\rho} = \begin{Bmatrix} R \cos \alpha \\ R \sin \alpha \\ z \end{Bmatrix}. \quad (64)$$

The necessary surface characteristics are the tangent vectors and the normal vector

$$\boldsymbol{\rho}_1 = \begin{Bmatrix} -R \sin \alpha \\ R \cos \alpha \\ 0 \end{Bmatrix}, \quad \boldsymbol{\rho}_2 = \begin{Bmatrix} 0 \\ 0 \\ 1 \end{Bmatrix}, \quad \mathbf{n} = \begin{Bmatrix} \cos \alpha \\ \sin \alpha \\ 0 \end{Bmatrix}, \quad (65)$$

resulting in a covariant surface metrics tensor

$$[a_{ij}] = \begin{bmatrix} (\boldsymbol{\rho}_1 \cdot \boldsymbol{\rho}_1) & (\boldsymbol{\rho}_1 \cdot \boldsymbol{\rho}_2) \\ (\boldsymbol{\rho}_2 \cdot \boldsymbol{\rho}_1) & (\boldsymbol{\rho}_2 \cdot \boldsymbol{\rho}_2) \end{bmatrix} = \begin{bmatrix} R^2 & 0 \\ 0 & 1 \end{bmatrix}. \quad (66)$$

Orthotropic properties of the surface are obtained as follows. The equation for a family of cylindrical spiral lines on the cylinder (64) is, see also the geometry given in Fig. 4:

$$\mathbf{r} = \begin{pmatrix} R \cos \alpha \\ R \sin \alpha \\ \frac{H}{2\pi} \alpha + \text{const} \end{pmatrix}. \quad (67)$$

The first tangent vector \mathbf{r}_1 along the spiral line necessary for the tensor representation (49) becomes:

$$\mathbf{r}_1 = \frac{\partial \mathbf{r}}{\partial \alpha} = \begin{pmatrix} -R \sin \alpha \\ R \cos \alpha \\ \frac{H}{2\pi} \end{pmatrix}. \quad (68)$$

The second tangent vector \mathbf{r}_2 is defined to be orthogonal to the first vector \mathbf{r}_1 and to the normal on the cylinder surface, see eqn. (65.3) and Fig. 4:

$$\mathbf{r}_2 = [\mathbf{n} \times \mathbf{r}_1] = \begin{pmatrix} \frac{H}{2\pi} \sin \alpha \\ -\frac{H}{2\pi} \cos \alpha \\ R \end{pmatrix}. \quad (69)$$

With this expression an equation for the line orthogonal to the main spiral line (67), see line **AC** in Fig. 4, can be found from the condition that the integrated and scaled tangent vector \mathbf{r}_2 must belong to the cylinder surface

$$A \int \mathbf{r}_2 d\alpha \in \text{cylinder} \implies A = \frac{2\pi R}{H}, \quad (70)$$

which leads to the following definition of a vector $\hat{\mathbf{r}}$, orthogonal to \mathbf{r} :

$$\hat{\mathbf{r}} = \begin{pmatrix} R \cos \alpha \\ R \sin \alpha \\ \frac{2\pi R^2}{H} \alpha + \text{const} \end{pmatrix}. \quad (71)$$

Thus, orthotropic properties are inherited from the orthogonal spiral net on the cylinder via eqns. (67) and (71).

Remark. For further analyses, one can define from eqns. (67) and (71) the distances between two adjacent threads as H for the main spiral and $\hat{H} = \frac{(2\pi R)^2}{H}$ for the orthogonal spiral **AC**, see Fig. 4.

The covariant components of the metric tensor g_{ij} are defined as

$$[g_{ij}] = \begin{bmatrix} R^2 + \left(\frac{H}{2\pi}\right)^2 & 0 \\ 0 & R^2 + \left(\frac{H}{2\pi}\right)^2 \end{bmatrix}. \quad (72)$$

The tensor of orthotropy \mathbf{B}^α in the Cartesian basis, see eqn. (49), becomes then:

$$\mathbf{B}^C = -\epsilon_1 \frac{\mathbf{r}_1 \otimes \mathbf{r}_1}{g_{11}} - \epsilon_2 \frac{\mathbf{r}_2 \otimes \mathbf{r}_2}{g_{22}} = \quad (73)$$

$$= -\frac{1}{R^2 + \left(\frac{H}{2\pi}\right)^2} \begin{bmatrix} g_\epsilon \sin^2 \alpha & -g_\epsilon \sin \alpha \cos \alpha & -(\epsilon_1 - \epsilon_2) \frac{RH}{2\pi} \sin \alpha \\ -g_\epsilon \sin \alpha \cos \alpha & g_\epsilon \cos^2 \alpha & (\epsilon_1 - \epsilon_2) \frac{RH}{2\pi} \cos \alpha \\ -(\epsilon_1 - \epsilon_2) \frac{RH}{2\pi} \sin \alpha & (\epsilon_1 - \epsilon_2) \frac{RH}{2\pi} \cos \alpha & \epsilon_1 \left(\frac{H}{2\pi}\right)^2 + \epsilon_2 R^2 \end{bmatrix},$$

with

$$g_\epsilon = \epsilon_1 R^2 + \epsilon_2 \left(\frac{H}{2\pi}\right)^2. \quad (74)$$

The backward tensor transformation (55) with the matrix \mathbf{H} defined via the cylindrical coordinates

$$\mathbf{H} = \begin{bmatrix} \frac{\partial x_i}{\partial \xi^j} \end{bmatrix} = \begin{bmatrix} \frac{\partial \boldsymbol{\rho}}{\partial \boldsymbol{\xi}} \end{bmatrix} = \begin{bmatrix} -R \sin \alpha & 0 \\ R \cos \alpha & 0 \\ 0 & 1 \end{bmatrix} \quad (75)$$

gives us the covariant components b_{ij} of the tensor \mathbf{B} in the contravariant surface basis $\boldsymbol{\rho}^1, \boldsymbol{\rho}^2$:

$$\mathbf{B} = [b_{ij}] = \mathbf{H}^T \mathbf{B}^C \mathbf{H} = -\frac{1}{R^2 + \left(\frac{H}{2\pi}\right)^2} \begin{bmatrix} g_\epsilon R^2 & (\epsilon_1 - \epsilon_2) \frac{R^2 H}{2\pi} \\ (\epsilon_1 - \epsilon_2) \frac{R^2 H}{2\pi} & \epsilon_1 \left(\frac{H}{2\pi}\right)^2 + \epsilon_2 R^2 \end{bmatrix}. \quad (76)$$

Matrix \mathbf{B} in eqn. (76) represents the constant spiral orthotropy for the cylindrical surface and, therefore, is a generalization of the constant plane orthotropy in eqn. (42) for the case of a cylindrical geometry.

Remark. With the assumption of isotropy $\epsilon_1 = \epsilon_2 = \epsilon$ the unit matrix is recovered only in mixed components. In covariant components we obtain

$$\mathbf{B}_{\epsilon_1=\epsilon_2=\epsilon} = [b_{ij}]_{\epsilon_1=\epsilon_2=\epsilon} = -\epsilon \begin{bmatrix} R^2 & 0 \\ 0 & 1 \end{bmatrix}. \quad (77)$$

s

4 Derivation of the frictional contact problem via the principle of maximum dissipation.

The principle of maximum dissipation is known in plasticity for the formulation of the necessary characteristics, such as plastic strains etc.. The application of this principle for the construction of computational algorithms in linear and nonlinear isotropic plasticity was developed in Simo and Hughes [29]. He and Curnier [12] formulated the dissipation function for the anisotropic function and investigated its extremal properties applying convex analysis. The correspondence between the dissipation function and the sliding rule was shown. Here we will also formulate the

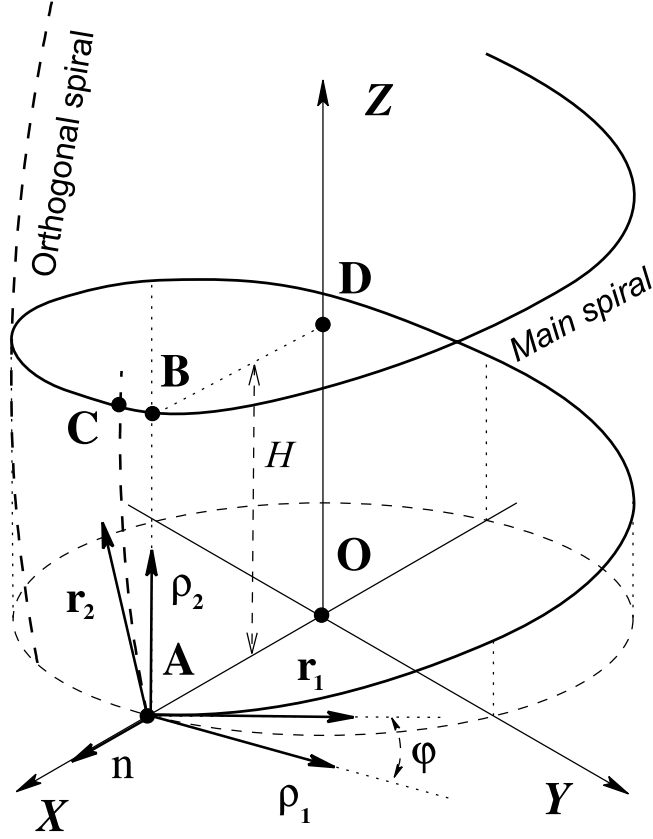


Figure 4: Spiral orthotropy on the cylindrical surface.

frictional problem as an extremal problem in a continuous form, and then applying the finite difference scheme in an incremental form. Afterwards, the return-mapping algorithm is applied to obtain all characteristics for sliding, such as a sliding force \mathbf{T}^{sl} and a sliding displacement vector $\Delta \boldsymbol{\xi}^{sl}$. These variables can be viewed as a pair of conjugate variables for the energy dissipation function, which allows to define them separately.

4.1 Continuous formulation

According to the elastic-plastic analogy, a frictional contact problem via the energy dissipation function can be formulated as follows:

- a) The relative velocity vector of the contact point is decomposed additively into an elastic part \mathbf{v}^{el} and a sliding part \mathbf{v}^{sl}

$$\mathbf{v}^r = \mathbf{v}^{el} + \mathbf{v}^{sl}. \quad (78)$$

- b) The elastic part \mathbf{v}^{el} is responsible for reversible deformations (adhesion) and satisfies the evolution equations (28):

$$\frac{d\mathbf{T}}{dt} = \mathbf{B}\mathbf{v}^{el}. \quad (79)$$

- c) The tangential force \mathbf{T} must satisfy the following inequalities defined via the yield function eqn. (33), which in tensor form can be written as:

$$\Phi := \sqrt{f^{ij}T_iT_j} - |N| = \sqrt{\mathbf{T} \cdot \mathbf{FT}} - |N| : \quad (80)$$

- if $\Phi < 0$ then the contact point is inside the elastic domain and $\mathbf{T} = \mathbf{T}^{el}$ is an elastic force,
- if $\Phi = 0$ then the contact point is sliding and $\mathbf{T} = \mathbf{T}^{sl}$ is a sliding force.

- d) The power of the sliding forces, described by the energy dissipation function D achieves its maximum:

$$D := \dot{\xi}_{sl}^i T_i^{sl} = \mathbf{v}^{sl} \cdot \mathbf{T}^{sl}, \quad D \longrightarrow \max. \quad (81)$$

For the convenient application of standard methods of convex analysis [21], [3], [11] we transform the problem (81) into a minimization problem

$$D_{min} := -\dot{\xi}_{sl}^i T_i^{sl} = -\mathbf{v}^{sl} \cdot \mathbf{T}^{sl}, \quad D_{min} \longrightarrow \min. \quad (82)$$

The principle of maximum dissipation requires that the plastic dissipation function D subjected to the inequality conditions (80) achieves a maximum. A system of ordinary equations (78) - (79) is defined in convective surface coordinates ξ^1, ξ^2 , identifying a contact point on the surface.

4.2 Incremental formulation

The application of the backward Euler scheme to the continuous problem a)-d) described above, namely to a system of ordinary differential equations (78)-(79) with an additional extremal condition (82) leads to an incremental formulation. Here we investigate only quasi-static contact problems, therefore we can take $\Delta t = 1$. The return-mapping scheme – for plasticity see [29] and among the first applications for contact problems see [8] – is applied to obtain the real sliding force and sliding displacements: the trial tangential force \mathbf{T}^{tr} is assumed to be elastic and can be computed from the incremental solution. Thus, the following incremental formulation for the trial tangential force \mathbf{T}^{tr} is found:

- i) The full displacement vector $\Delta \boldsymbol{\xi} = \boldsymbol{\xi}^{(n+1)} - \boldsymbol{\xi}^{(n)}$ is decomposed additively into an elastic increment $\Delta \boldsymbol{\xi}^{el}$ and into a sliding increment $\Delta \boldsymbol{\xi}^{sl}$:

$$\Delta \boldsymbol{\xi} = \Delta \boldsymbol{\xi}^{el} + \Delta \boldsymbol{\xi}^{sl}, \quad (83)$$

where both vectors are defined in the surface metrics, namely,

$$\Delta \boldsymbol{\xi} := \Delta \xi^i \boldsymbol{\rho}_i = (\xi_{(n+1)}^i - \xi_{(n)}^i) \boldsymbol{\rho}_i. \quad (84)$$

- ii) The trial force $\mathbf{T}_{(n+1)}^{tr}$ is computed via the incremental evolution equations:

$$\mathbf{T}_{(n+1)}^{tr} - \mathbf{T}_{(n)} = \mathbf{B}^{(n+1)}(\boldsymbol{\xi}_{(n+1)}^{el} - \boldsymbol{\xi}_{(n)}^{el}). \quad (85)$$

iii) In order to decide whether the trial force \mathbf{T}^{tr} is a sliding force \mathbf{T}^{sl} or a sticking force \mathbf{T}^{st} the yield condition is checked in each load step:

$$\begin{aligned}\Phi^{tr} &:= \sqrt{\mathbf{T}_{(n+1)}^{tr} \cdot \mathbf{F}_{(n+1)} \mathbf{T}_{(n+1)}^{tr}} - |N_{(n+1)}| \\ &= \sqrt{f^{ij} T_{i(n+1)}^{tr} T_{j(n+1)}^{tr}} - |N_{(n+1)}|,\end{aligned}\quad (86)$$

- If $\Phi^{tr} < 0$ then the trial force is a real sticking force $\mathbf{T} = \mathbf{T}^{tr}$.
- If $\Phi^{tr} \geq 0$ then the sliding force must be obtained via the maximum of the energy dissipation function given in the incremental form.

iv) The incremental analog of the continuous formulation eqn. (82) is then:

$$D_{min}^{(n+1)} := -\Delta \boldsymbol{\xi}^{sl} \cdot \mathbf{T}_{(n+1)}^{sl} = -\Delta \xi_{sl}^i T_{i(n+1)}^{sl}, \quad D_{min}^{(n+1)} \longrightarrow \min. \quad (87)$$

For large sliding problems especially with reversible loading, it is necessary to define both, the sliding force and the sliding displacements. Taking the sliding distance $\Delta \boldsymbol{\xi}_{sl}$ as an independent variable we can determine the sliding force \mathbf{T}^{sl} via the minimum of the function $D_{min}^{(n+1)}$ in eqn. (87). The expression for the sliding force will be used for numerical computation within each load step during an iterative Newton solution scheme. The sliding distance, in due course, is defined after convergence is achieved in the load step and is computed via the consistency condition.

A *Lagrange function* for the constraint minimization problem is given as:

$$\begin{aligned}\mathcal{L}_{(n+1)} &:= -\Delta \boldsymbol{\xi}^{sl} \cdot \mathbf{T}_{(n+1)}^{sl} + \lambda \left(\sqrt{\mathbf{T}_{(n+1)}^{tr} \cdot \mathbf{F}_{(n+1)} \mathbf{T}_{(n+1)}^{tr}} - |N_{(n+1)}| \right), \\ \mathcal{L} &\longrightarrow \min,\end{aligned}\quad (88)$$

where the complementary Kuhn-Tucker conditions (see [21], [3]) are given as:

$$\Phi := \sqrt{\mathbf{T}_{(n+1)}^{tr} \cdot \mathbf{F}_{(n+1)} \mathbf{T}_{(n+1)}^{tr}} - |N_{(n+1)}| \leq 0, \quad \lambda \geq 0, \quad \lambda \Phi_{(n+1)} = 0. \quad (89)$$

For the next transformations a gradient of the yield function is necessary:

$$\frac{\partial \Phi_{(n+1)}}{\partial \mathbf{T}_{(n+1)}^{tr}} = \frac{\mathbf{F}_{(n+1)} \mathbf{T}_{(n+1)}^{tr}}{\sqrt{\mathbf{T}_{(n+1)}^{tr} \cdot \mathbf{F}_{(n+1)} \mathbf{T}_{(n+1)}^{tr}}}, \quad (90)$$

as well as a derivative of the trial force at load step $(n+1)$, computed via the chain rule, see eqns. (85) and (83):

$$\frac{\partial \mathbf{T}_{(n+1)}^{tr}}{\partial \Delta \boldsymbol{\xi}^{sl}} = -\mathbf{B}_{(n+1)}. \quad (91)$$

In the following sections the subscript $(n+1)$ will be omitted everywhere for simplicity reasons.

4.2.1 Derivation of the sliding force \mathbf{T}^{sl} .

In order to obtain the sliding force \mathbf{T}^{sl} , the sliding incremental displacement $\Delta\xi^{sl}$ is taken as an independent variable. A formal application of convex analysis, see [21], [3], to the Lagrange function (88) gives us the necessary condition of the minimum:

$$\frac{\partial \mathcal{L}}{\partial \Delta\xi^{sl}} = 0, \quad (92)$$

leading to the definition of the sliding force as:

$$\mathbf{T}^{sl} = \lambda \frac{\partial \Phi}{\partial \Delta\xi^{sl}}. \quad (93)$$

Exploiting the chain rule and using eqns. (90), (91), we obtain:

$$\mathbf{T}^{sl} = \lambda \frac{\partial \Phi}{\partial \mathbf{T}^{tr}} \frac{\partial \mathbf{T}^{tr}}{\partial \Delta\xi^{sl}} = -\lambda \mathbf{B} \frac{\mathbf{F}\mathbf{T}^{tr}}{\sqrt{\mathbf{T}^{tr} \cdot \mathbf{F}\mathbf{T}^{tr}}}. \quad (94)$$

For the current sliding case, i.e. when $\lambda > 0$, we have to satisfy the Kuhn-Tucker condition $\Phi = 0$, in order to define λ , i.e. substitute \mathbf{T}^{sl} in the yield function $\Phi = \sqrt{\mathbf{T}^{sl} \cdot \mathbf{F}\mathbf{T}^{sl}} - |N|$. This leads to the following equation for λ :

$$\lambda = |N| \sqrt{\frac{\mathbf{T}^{tr} \cdot \mathbf{F}\mathbf{T}^{tr}}{\mathbf{B}\mathbf{F}\mathbf{T}^{tr} \cdot \mathbf{F}\mathbf{B}\mathbf{F}\mathbf{T}^{tr}}}, \quad (95)$$

where the positive λ is taken due to the second Kuhn-Tacker condition in eqn. (89). Thus, the sliding force \mathbf{T}^{sl} in eqn. (94) is defined as

$$\mathbf{T}^{sl} = -\frac{\mathbf{B}\mathbf{F}\mathbf{T}^{tr}}{\sqrt{\mathbf{B}\mathbf{F}\mathbf{T}^{tr} \cdot \mathbf{F}\mathbf{B}\mathbf{F}\mathbf{T}^{tr}}} |N|. \quad (96)$$

We now introduce an auxiliary vector

$$\hat{\mathbf{T}} = \mathbf{B}\mathbf{F}\mathbf{T}^{tr} \quad (97)$$

to compute the sliding force \mathbf{T}^{sl} . The covariant components of the auxiliary vector are defined via various components of the tensor \mathbf{B} and \mathbf{F} as:

$$\hat{T}_i = b_{ij} f^{jk} T_k^{tr} = b_{ij} f_{ln} a^{jl} a^{kn} T_k^{tr} = b_i^j f_j^k T_k^{tr}. \quad (98)$$

Then the covariant components of the sliding vector (96) can be computed as

$$\mathbf{T}^{sl} = -\frac{\hat{\mathbf{T}}}{\sqrt{\hat{\mathbf{T}} \cdot \mathbf{F}\hat{\mathbf{T}}}} \implies T_i^{sl} = -\frac{\hat{T}_i}{\sqrt{\hat{T}_k \hat{T}_l f^{kl}}} \quad (99)$$

The isotropic case is recovered from eqn. (96) by taking $\mathbf{B} = -\epsilon_T \mathbf{E}$ and $\mathbf{F} = \mathbf{E}/\mu^2$ to

$$\mathbf{T}^{sl} = \mu |N| \frac{\mathbf{T}^{tr}}{\sqrt{\mathbf{T}^{tr} \cdot \mathbf{T}^{tr}}}. \quad (100)$$

4.3 Specification of initial conditions for the return-mapping scheme.

Initial conditions are necessary for the incremental solution of eqns.(83) and (85) formulated as Cauchy problem for a system of ordinary differential equations. These initial conditions can be defined assuming that the initial configuration is unstressed, thus with zero external loading:

$$\mathbf{T} = 0, N = 0 \implies \boldsymbol{\xi} = \boldsymbol{\xi}_{(0)}, \boldsymbol{\xi}_{(0)}^{sl} = 0 \text{ for } \xi^3 \leq 0. \quad (101)$$

The conditions are formulated for all points which are in contact at the initial configuration, i.e. for all points satisfying $\xi^3 \leq 0$. The vector $\boldsymbol{\xi}_{(0)}$ is obtained via a projection procedure, and defines the center of the ellipse for the adhesion domain, see Fig. 5. The additional initialization of the sliding displacement and the update procedure will be discussed after the geometrical interpretation of the solution process.

4.4 Derivation of the sliding incremental displacement $\Delta \boldsymbol{\xi}^{sl}$ and update scheme for the history variables.

We consider here a "step-by-step" scheme for the case with nonlinear tensors \mathbf{B} and \mathbf{F} concentrating on computational aspects for the numerical implementation. For the nonlinear case let us assume that the first converged load step is elastic, i.e. $\Phi < 0$ in eqn. (89), while for the second load step the sliding condition is achieved, i.e. $\Phi = 0$ and the load step was computed with the sliding force \mathbf{T}^{sl} . Let $\boldsymbol{\xi}_{(1)}$ and $\boldsymbol{\xi}_{(2)}$ are convective coordinates of a contact point after the corresponding first and the second load steps. The trial force for the second load step $\mathbf{T}_{(2)}^{tr}$ is then computed as in an Euler backward scheme:

$$\mathbf{T}_{(2)}^{tr} = \mathbf{T}_{(1)} + \mathbf{B}^{(2)}(\boldsymbol{\xi}_{(2)} - \boldsymbol{\xi}_{(1)}), \quad (102)$$

where for the first load step a force $\mathbf{T}_{(1)}$ is computed taking into account the initial conditions in eqn. (101)

$$\mathbf{T}_{(1)} = \mathbf{B}^{(1)}(\boldsymbol{\xi}_{(1)} - \boldsymbol{\xi}_{(0)}). \quad (103)$$

The value of the sliding displacement $\boldsymbol{\xi}_{(2)}^{sl}$ and resp. the elastic part $\boldsymbol{\xi}_{(2)}^{el}$ are defined via the strict fulfillment of the Kuhn-Tucker condition $\Phi_{(2)} = 0$ for the elastic part $\boldsymbol{\xi}_{(2)}^{el}$:

$$\begin{aligned} \Phi_{(2)} = \Phi_{(2)}(\boldsymbol{\xi}, \boldsymbol{\xi}^{sl}) = \\ \sqrt{(\mathbf{T}_{(1)} + \mathbf{B}^{(2)}(\boldsymbol{\xi}_{(2)}^{el} - \boldsymbol{\xi}_{(1)})) \cdot \mathbf{F}^{(2)}(\mathbf{T}_{(1)} + \mathbf{B}^{(2)}(\boldsymbol{\xi}_{(2)}^{el} - \boldsymbol{\xi}_{(1)}))} - |N|, \end{aligned} \quad (104)$$

where the full displacement vector $\boldsymbol{\xi}_{(2)}$ after the converged second load step can be decomposed as:

$$\boldsymbol{\xi}_{(2)} = \boldsymbol{\xi}_{(2)}^{el} + \boldsymbol{\xi}_{(2)}^{sl}. \quad (105)$$

The consistency condition (see [21], [3]) for the constraint function $\Phi_{(2)}$ leads to an additional equation allowing to determine the direction of the sliding displacement:

$$\dot{\Phi} = \frac{\partial \Phi}{\partial \boldsymbol{\xi}_{(2)}} \cdot \frac{d\boldsymbol{\xi}_{(2)}}{dt} + \frac{\partial \Phi}{\partial \boldsymbol{\xi}_{(2)}^{sl}} \cdot \frac{d\boldsymbol{\xi}_{(2)}^{sl}}{dt} = 0. \quad (106)$$

Continuing with the chain rule we obtain:

$$\frac{\partial \Phi}{\partial \boldsymbol{\xi}_{(2)}^{el}} \frac{\partial \boldsymbol{\xi}_{(2)}^{el}}{\partial \boldsymbol{\xi}_{(2)}} \cdot \frac{d\boldsymbol{\xi}_{(2)}}{dt} + \frac{\partial \Phi}{\partial \boldsymbol{\xi}_{(2)}^{el}} \frac{\partial \boldsymbol{\xi}_{(2)}^{el}}{\partial \boldsymbol{\xi}_{(2)}^{sl}} \cdot \frac{d\boldsymbol{\xi}_{(2)}^{sl}}{dt} = \frac{\partial \Phi}{\partial \boldsymbol{\xi}_{(2)}^{el}} \cdot \left(\frac{d\boldsymbol{\xi}_{(2)}}{dt} - \frac{d\boldsymbol{\xi}_{(2)}^{sl}}{dt} \right) = 0. \quad (107)$$

From the last equation, we can obtain the following condition

$$\frac{d\boldsymbol{\xi}_{(2)}^{sl}}{dt} = \frac{d\boldsymbol{\xi}_{(2)}}{dt}. \quad (108)$$

Then the sliding displacement update vector $\boldsymbol{\xi}_{(2)}^{sl}$ can be defined in the direction of the last converged full displacement vector $\boldsymbol{\xi}_{(2)}$. For the computation of the nonlinear case this direction can be approximately taken as

$$\mathbf{e} = \frac{\boldsymbol{\xi}_{(2)} - \boldsymbol{\xi}_{(1)}}{|\boldsymbol{\xi}_{(2)} - \boldsymbol{\xi}_{(1)}|} \quad (109)$$

leading to the sliding displacement

$$\boldsymbol{\xi}_{(2)}^{sl} = \lambda \mathbf{e}. \quad (110)$$

Parameter λ defining the length of the vector is obtained from the Kuhn-Tucker condition for the function $\Phi_{(2)}$ in eqn. (104). This leads to the following algebraic equation:

$$\begin{aligned} \lambda^2 (\mathbf{B}^{(2)} \mathbf{e} \cdot \mathbf{F}^{(2)} \mathbf{B}^{(2)} \mathbf{e}) - 2\lambda (\mathbf{B}^{(2)} \mathbf{e} \cdot \mathbf{F}^{(2)} \mathbf{T}_{(2)}) + \\ + \mathbf{T}_{(2)} \cdot \mathbf{F}^{(2)} \mathbf{T}_{(2)} - N^2 = 0, \end{aligned} \quad (111)$$

where the positive root $\lambda > 0$, minimizing globally the function in eqn. (87), should be taken.

4.5 Computational aspects for further implementation considering nonlinear and constant tensors.

For the further implementations we consider the following cases: a) with nonlinear tensors for large displacement problems; b) with constant tensors, i.e. the case of constant orthotropy.

4.5.1 A case with nonlinear tensors for large displacement problems

Within the adjustment of the sliding force the strict execution of the backward scheme in eqn. (85) leads to the necessity to store as history variables in addition to $\boldsymbol{\xi}_{(n)}^{el}$ also updated sliding variables $\boldsymbol{\xi}_{(n)}^{sl}$ at load step (n), which is computationally rather expensive. However, the numerical experience from some cases even with non-constant \mathbf{B} , e.g. for polar orthotropy, shows that it may be mostly sufficient to use a simplified scheme, which is identical with the backward scheme computed with the updated matrix $\mathbf{B}^{(n+1)}$ at load step ($n+1$), namely, with the following finite difference scheme:

$$\mathbf{T}_{(n+1)}^{tr} = \mathbf{T}_{(n)} + \mathbf{B}^{(n+1)}(\boldsymbol{\xi}_{(n+1)} - \boldsymbol{\xi}_{(n)}), \quad (112)$$

where $\boldsymbol{\xi}_{(n)}$ is a displacement vector from the converged load step (n). For large displacement problems the elastic part $\boldsymbol{\xi}^{el}$ can be neglected leading to the result that the update sliding vector $\boldsymbol{\xi}_{(n)}^{sl}$ is equal to the displacement vector $\boldsymbol{\xi}_{(n)}$ in the last converged load step. Computations show that the scheme in eqn. (112) is robust and requires only $\mathbf{T}_{(n)}$ and $\boldsymbol{\xi}_{(n)}$ as history variables.

4.5.2 A case with constant orthotropy

For the case with a constant tensor \mathbf{B} , we can proceed recursively transforming eqn. (85) similar to the isotropic case, see eqn. (13), and obtain

$$\begin{aligned} \mathbf{T}_{(n+1)}^{tr} = \mathbf{T}_{(n)} + \mathbf{B} \Delta \boldsymbol{\xi}^{el} = \dots = \mathbf{B}(\Delta \boldsymbol{\xi}_{(n+1)} - \Delta \boldsymbol{\xi}^{sl}), \\ \Delta \boldsymbol{\xi}_{(n+1)} = \boldsymbol{\xi}_{(n+1)} - \boldsymbol{\xi}_{(0)}, \end{aligned} \quad (113)$$

where $\boldsymbol{\xi}_{(0)}$ is a center of the elliptical adhesion domain, for which a geometrical interpretation is given later.

For the case with constant tensors the update algorithm in Sect. 4.4 leads to the exact definition of the sliding displacement as:

$$\Delta\boldsymbol{\xi}^{sl} = \boldsymbol{\xi} - \boldsymbol{\xi}^{(0)} - |N| \frac{\boldsymbol{\xi} - \boldsymbol{\xi}^{(0)}}{\sqrt{(\boldsymbol{\xi} - \boldsymbol{\xi}^{(0)}) \cdot \mathbf{BFB}(\boldsymbol{\xi} - \boldsymbol{\xi}^{(0)})}}, \quad (114)$$

where $\boldsymbol{\xi}$ is the full displacement vector after the converged load step. A geometrical interpretation of this scheme is discussed in the next section.

4.6 Geometrical interpretation of the solution process.

A simple geometrical interpretation for the solution can be given for a plane surface with constant orthotropy in the case of both, elastic sticking and sliding behavior. Interpretations can be formulated in the trial force space T_1^{tr}, T_2^{tr} and on the tangent plane ξ^1, ξ^2 where we assume Cartesian metrics, i.e. $a_{ij} = \delta_{ij}$. In the trial force space the yield function in eqn. (86) represents an ellipse due to the positivity of the friction tensor \mathbf{F} :

$$\mathbf{T}^{tr} \cdot \mathbf{F}\mathbf{T}^{tr} = N^2. \quad (115)$$

In order to obtain the interpretation on the tangent plane, the incremental evolution equation (113) is used. Then, we also obtain an ellipse on the tangent plane

$$\mathbf{B}\Delta\boldsymbol{\xi} \cdot \mathbf{F}\mathbf{B}\Delta\boldsymbol{\xi} = N^2. \quad (116)$$

In order to derive further characteristics, the symmetrical tensors \mathbf{F} and \mathbf{B} are expressed via the spectral representation (41):

$$\mathbf{B} = \mathbf{Q}_\alpha \mathbf{D}_B \mathbf{Q}_\alpha^T, \quad \mathbf{F} = \mathbf{Q}_\beta \mathbf{D}_F \mathbf{Q}_\beta^T, \quad (117)$$

where \mathbf{Q}_α and \mathbf{Q}_β are rotational matrices with corresponding angles α and β , see eqn. (40), and $\mathbf{D}_B, \mathbf{D}_F$ are diagonal matrices:

$$\mathbf{D}_B = - \begin{bmatrix} \varepsilon_1 & 0 \\ 0 & \varepsilon_2 \end{bmatrix}, \quad \mathbf{D}_F = \begin{bmatrix} \frac{1}{\mu_1^2} & 0 \\ 0 & \frac{1}{\mu_2^2} \end{bmatrix}. \quad (118)$$

Spectral representations leads to the canonical form of ellipses. Thus, eqn. (115) becomes then

$$\mathbf{Q}_\beta^T \mathbf{T}^{tr} \cdot \begin{bmatrix} \frac{1}{\mu_1^2 N^2} & 0 \\ 0 & \frac{1}{\mu_2^2 N^2} \end{bmatrix} \mathbf{Q}_\beta^T \mathbf{T}^{tr} = 1, \quad (119)$$

describing a central ellipse inclined with angle β in the force plane T_1^{tr}, T_2^{tr} with the main axes $\mu_i N$.

Eqn. (116) describes a domain with orthotropic elastic properties, where the contact point S is attracted by the center (adhesion domain). Its transformation according to the representation (117) and (118) gives the following canonical equation:

$$(\mathbf{Q}_\alpha \mathbf{Q}_\alpha \mathbf{Q}_\beta^T)^T \Delta \boldsymbol{\xi} \cdot \begin{bmatrix} 1 & 0 \\ \frac{1}{(\mu_1 N / \varepsilon_1)^2} & 1 \\ 0 & \frac{1}{(\mu_2 N / \varepsilon_2)^2} \end{bmatrix} (\mathbf{Q}_\alpha \mathbf{Q}_\alpha \mathbf{Q}_\beta^T)^T \Delta \boldsymbol{\xi} = 1, \quad (120)$$

$$\Delta \boldsymbol{\xi} = \boldsymbol{\xi}_{(n+1)} - \boldsymbol{\xi}_{(0)}$$

describing an ellipse inclined by the matrix $\mathbf{Q}_\alpha \mathbf{Q}_\alpha \mathbf{Q}_\beta^T$. The ellipse center is shifted by the distance $\boldsymbol{\xi}_{(0)}$ on the tangent plane ξ^1, ξ^2 , see Fig. 5. The lengths of the main axes of the ellipse are a resp. $b = \mu_i N / \varepsilon_i$. The inclination angle becomes $\phi = 2\alpha - \beta$, which is verified from the matrix:

$$\mathbf{Q}_\alpha \mathbf{Q}_\alpha \mathbf{Q}_\beta^T = \begin{bmatrix} \cos(2\alpha - \beta) & -\sin(2\alpha - \beta) \\ \sin(2\alpha - \beta) & \cos(2\alpha - \beta) \end{bmatrix} \quad (121)$$

In the numerical examples, we will also investigate a case with nonlinear orthotropy with

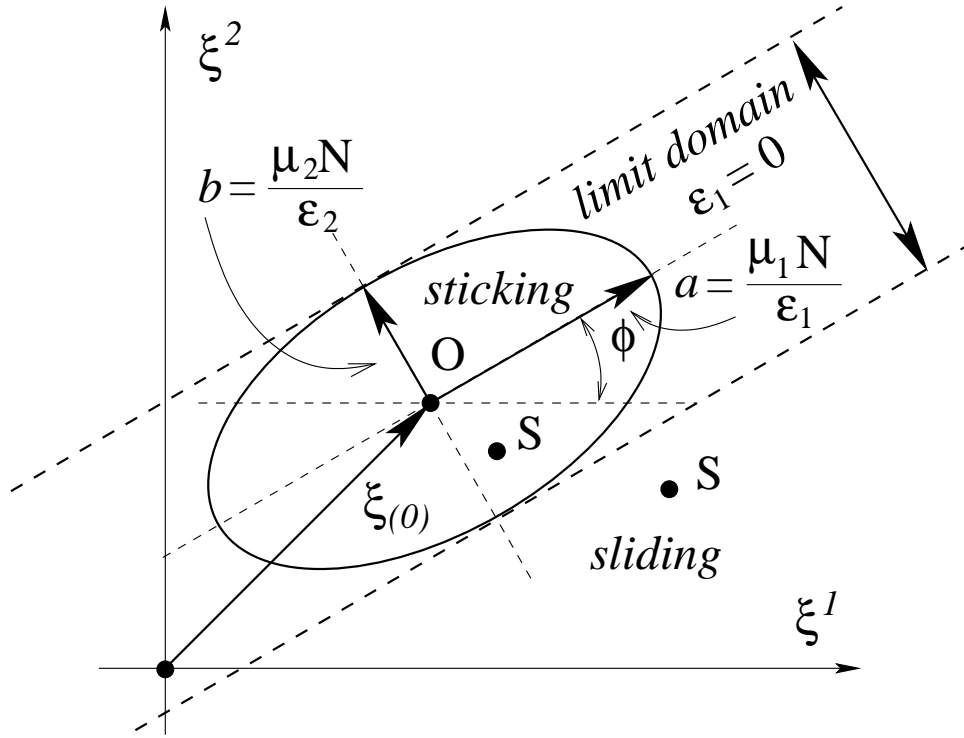


Figure 5: Allowable elastic region (adhesion domain).

$\varepsilon_1 = 0$. In this limit case with $\lim a = \infty$ the ellipse degenerates into an infinite strip of width $2b = 2 \frac{\mu_2 N}{\varepsilon_2}$, see Fig. 5. The properties inside the strip defined by eqn. (113) are elastic, but the motion along the strip causes the corresponding elastic force to be zero $T_a = 0$.

Thus, a *geometrical interpretation of the solution* is as follows. The ellipse describes an elastic domain with orthotropic properties obtained by the incremental evolution equation (113). The sticking condition is fulfilled when a contact point S remains inside the ellipse. If a contact point S appears outside of the ellipse, then this point is sliding, i.e. the acting force is

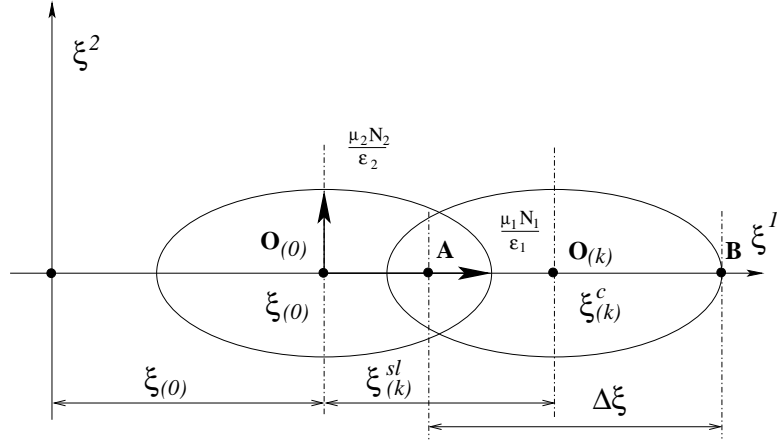


Figure 6: Update scheme. Particular case.

computed via eqn. (99), see Fig. 5. Due to the condition $\Phi = 0$ this point is on the boundary of the elliptic region, which leads to a shifting of the ellipse in order to define the forces in the next load step correctly. This shifting is originated by the sliding vector $\Delta \boldsymbol{\xi}^{sl}$ which leads to an update of the ellipse center and which is computed via the update scheme in eqn. (114). The ellipse center is an attraction point for the domain with anisotropic elastic central forces defined by the evolution equation (113). As long as the contact point S is inside of the adhesion domain, the sliding displacements as well as the sliding forces have not to be computed. This is, the so-called, "sticking zone". Let k be the number of the load step, when sliding is detected the first time, i.e. the contact point has been moved outside the adhesion domain. Then, the sliding displacement $\boldsymbol{\xi}_{(k)}^{sl}$ is computed via eqn. (114). Now, the trial procedure in eqn. (113) is considered in the next load step ($k + 1$). Since the trial procedure is a computation in the elastic region, the sliding displacement $\boldsymbol{\xi}_{(k+1)}^{sl}$ is assumed to be zero.

$$\begin{aligned}
\mathbf{T}_{(k+1)}^{tr} &= \mathbf{B}(\Delta \boldsymbol{\xi}_{(k+1)} - \Delta \boldsymbol{\xi}_{(k+1)}^{sl}) = \\
&= \mathbf{B}(\boldsymbol{\xi}_{(k+1)} - \boldsymbol{\xi}_{(0)} - \boldsymbol{\xi}_{(k)}^{sl}) = \\
&= \mathbf{B}(\boldsymbol{\xi}_{(k+1)} - \underbrace{(\boldsymbol{\xi}_{(0)} + \boldsymbol{\xi}_{(k)}^{sl})}_{\boldsymbol{\xi}_{(k)}^c}).
\end{aligned} \tag{122}$$

Vector $\boldsymbol{\xi}_{(k)}^c$ defines the update scheme for the sliding displacements and allows to describe the shift of the ellipse center. The incremental evolution equation (113) is corrected then in accordance to this update scheme as

$$\begin{aligned}
\mathbf{T}_{(n+1)}^{tr} &= \mathbf{B}(\Delta \boldsymbol{\xi}_{(n+1)} - \boldsymbol{\xi}_n^c), \\
\text{with } \boldsymbol{\xi}_n^c &= \boldsymbol{\xi}_{n-1}^c + \boldsymbol{\xi}_n^{sl} = \dots = \boldsymbol{\xi}^0 + \boldsymbol{\xi}_k^c + \dots + \boldsymbol{\xi}_n^{sl}.
\end{aligned} \tag{123}$$

Now a particular case is considered, when the orthotropy axes coincide with the Cartesian coordinate axes (i.e. $\mathbf{Q}_\alpha = \mathbf{Q}_\beta = \mathbf{E}$) and a contact point being at the position \mathbf{A} during the load step (k) moved to the position \mathbf{B} during the load step ($k + 1$) along the ξ^1 axis with the distance $\Delta \xi$, see Fig. 6. In this case, the trial force is obtained as $T_1^{tr} = -\varepsilon_1 \Delta \xi$, and the following sliding displacement $\Delta \xi^{sl}$ in eqn. (114) becomes then

$$\Delta \xi^{sl} = \Delta \xi - |N| \frac{\Delta \xi \mu_1}{\sqrt{(\Delta \xi \varepsilon_1)^2}} = \frac{T_1^{tr}}{\varepsilon_1 |T_1^{tr}|} (-|T_1^{tr}| + \mu_1 |N|). \tag{124}$$

From Fig. 6 it becomes obvious that the sliding displacement $\Delta\xi^{sl}$ is updating the position of the ellipse center \mathbf{O} . The last result (124) can already be found for the isotropic case in Wriggers and Krstulovic-Opara [34] and [16]. In addition, the analogy between the geometrical interpretations of friction and plasticity with kinematical hardening, as described in Simo and Hughes [29] becomes obvious.

5 Conclusion

In this contribution a model for anisotropic surfaces including both anisotropy for adhesion and anisotropy for friction domains has been developed. The principle of maximum dissipation is applied to derive all necessary parameters. The problem is formulated in a covariant form in the surface coordinate system. Various types of anisotropy based either on the spectral decomposition, or inherited from the arbitrary curvilinear coordinate system are considered. As an example, the adhesion tensor and the friction tensor are derived for the polar orthotropy on a plane and the spiral orthotropy on a cylinder. A special attention is paid to the geometrical interpretation of the solution process. The current consideration is the necessary step for an iterative Newton type solution within the finite element method. The subsequent linearization procedure, details of the finite element implementation and numerical examples will be considered in the second part.

References

- [1] Araki, Y., Hjelmstad, K. D. Rate-dependent projection operators for frictional contact constraints. *International Journal for Numerical Methods in Engineering*. **57** (2003) 923–954.
- [2] Bandeira, A. A., Wriggers, P., Pimenta, P. M. Numerical derivation of contact mechanics interface laws using a finite element approach for large 3D deformation. *International Journal for Numerical Methods in Engineering*. **59** (2004) 173–195.
- [3] Borwein, J. M., Lewis, A. S. *Convex analysis and nonlinear optimization. Theory and examples* (Springer: New York, Heidelberg, 2000).
- [4] Buczkowski, R., Kleiber, M. Elasto-plastic interface model for 3D-frictional orthotropic contact problems. *International Journal for Numerical Methods in Engineering*. **40** (1997) 599–619.
- [5] Buczkowski, R., Kleiber, M. A stochastic model of rough surfaces for finite element contact analysis. *Computer Methods in Applied Mechanics and Engineering*. **199** (1999) 43–59.
- [6] Buczkowski, R., Kleiber, M. Statistical model of strongly anisotropic rough surfaces for finite element contact analysis. *International Journal for Numerical Methods in Engineering*. **49** (2000) 1169–1189.
- [7] Curnier, A. A theory of friction. *International Journal of Solids and Structures*. **20** (1984) 637–647.
- [8] Giannakopoulos, A. E. The return mapping method for the integration of friction constitutive relations. *Computers and Structures*. **32** (1989) 157–167.
- [9] Greenwood, J. A., Williamson, J. B. P. Contact of nominally flat surfaces. *Proc. of the Royal Society of London. Series A, Mathematical and Physical Sciences*. **295** (1966) 300–319.
- [10] Greenwood, J. A. A unified theory of surfaces roughness. *Proc. of the Royal Society of London. Series A, Mathematical and Physical Sciences*. **393** (1984) 133–157.
- [11] Glowinski, R., Lions, J.-L. Tremolieres, R. Numerical analysis of variational inequalities, Rev. edition, (Amsterdam: North-Holland, 1981).
- [12] He, Q.-C., Curnier, A. Anisotropic dry friction between two orthotropic surfaces undergoing large displacements. *European Journal of Mechanics A/Solids*. **12** (1993) 631–666.
- [13] Hjjaj, M., Feng, Z.-Q., de Saxce, G., Mroz, Z. Three-dimensional finite element computations for frictional contact problems with non-associated sliding rule. *International Journal for Numerical Methods in Engineering*. **60** (2004) 2045–2076.
- [14] Konyukhov A., Schweizerhof K. Contact formulation via a velocity description allowing efficiency improvements in frictionless contact analysis. *Computational Mechanics*. **33** (2004) 165–173.
- [15] Konyukhov A., Schweizerhof K. Covariant description for frictional contact problems. *Computational Mechanics*. **35** (2005) 190–213.

- [16] Krstulovic-Opara, L., Wriggers, P., Korelc J. A C^1 -continuous formulation for 3D finite deformation frictional contact. *Computational Mechanics*. **29** (2002) 27–42.
- [17] Krstulovic-Opara, L., Wriggers, P. A two-dimensional C^1 -continuous contact element based on the moving friction cone description. *WCCM V. Fifth World Congress on Computational Mechanics*. (2002, Vienna, Austria).
- [18] Laursen, T.A., Simo, J.C. A continuum-based finite element formulation for the implicit solution of multibody large deformation frictional contact problems. *International Journal for Numerical Methods in Engineering*. **35** (1993) 3451–3485.
- [19] Laursen, T. A. *Computational Contact and Impact Mechanics. Fundamentals of Modeling Interfacial Phenomena in Nonlinear Finite Element Analysis* (Springer: New-York, Heidelberg, Paris, 2002).
- [20] Longuet-Higgins M. S. The statistical analysis of a random, moving surface. *Proc. of the Royal Society of London. Series A, Mathematical and Physical Sciences*. **249** (1957) 321–387.
- [21] Luenberger, D. G. *Linear and Nonlinear programming* 2nd ed., Addison-Wesley, (1984).
- [22] McCool, John I. Comparison of models for the contact of rough surfaces. *Wear*. **107** (1986) 37–60.
- [23] Michalowski, R., Mroz, Z. Associated and non-associated sliding rules in contact friction problems. *Archives of Mechanics. (Archiwum mechaniki stosowanej), Polish Academy of Sciences*. **30** (1978) 259–276.
- [24] Mroz, Z., Stupkiewicz, S. An anisotropic friction and wear model. *International Journal of Solids and Structures*. **31** (1994) 1113–1131.
- [25] Oancea, V. G., Laursen, T. A. On the constitutive modeling and finite element computation of rate-dependent frictional sliding in large deformations. *Computer Methods in Applied Mechanics and Engineering*. **143** (1997) 197–227.
- [26] Jones, R.E., Papadopoulos, P. Simulating anisotropic frictional response using smoothly interpolated traction fields. *Computer Methods in Applied Mechanics and Engineering*. (Available online 3 June 2005).
- [27] Parisch, H., Lübbing, Ch. A formulation of arbitrarily shaped surface elements for three-dimensional large deformation contact with friction. *International Journal for Numerical Methods in Engineering*. **40** (1997) 3359–3383.
- [28] Peric, D., Owen, D. R. J. Computational model for 3-D contact problems with friction based on the penalty method. *International Journal for Numerical Methods in Engineering*. **35** (1992) 1289–1309.
- [29] Simo, J.C., Hughes, T.J.R. *Elastoplasticity and Viscoplasticity: computational aspects*, Springer-Verlag: Berlin, (1992).
- [30] Whitehouse, D. J., Archard, J. F. The properties of random surfaces of significance in their contact. *Proc. of the Royal Society of London. Series A, Mathematical and Physical Sciences*. **316** (1970) 97–121.

- [31] Whitehouse, D. J., Phillips, M. J. Two-dimensional discrete properties of random surfaces. *Proc. of the Royal Society of London. Series A, Mathematical and Physical Sciences.* **305** (1982) 441–468.
- [32] Wriggers, P., Vu Van, Stein E. Finite element formulation of large deformation impact-contact problems with friction. *Computers and Structures.* **37** (1990) 319–331.
- [33] Wriggers, P. *Computational Contact Mechanics*, John Wiley & Sons: Chichester (2002).
- [34] Wriggers, P., Krstulovic-Opara, L., Korelc J. Smooth C^1 -interpolations for two-dimensional frictional contact problems. *International Journal for Numerical Methods in Engineering.* **51** (2001) 1469–1495.
- [35] Wriggers, P., Zavarise, G. Thermomechanical contact – a rigorous but simple numerical approach. *Computer and Structures.* **46** (1993) 47–53.
- [36] Wriggers, P., Zavarise, G. On the application of Augmented Lagrangian techniques for nonlinear constitutive laws in contact interface. *Communications in Applied Numerical Methods.* **9** (1993) 815–824.
- [37] Zavarise, G., Wriggers, P., Stein, E., Schrefler, B. A numerical model for thermomechanical contact based on microscopic interface laws. *Mechanics Research Communications.* **19** (1992) 173–182.
- [38] Zmitrowicz, A. A theoretical model of anisotropic dry friction. *Wear.* **73** (1981) 9–39.
- [39] Zmitrowicz, A. Mathematical description of anisotropic friction. *International Journal of Solids and Structures.* **25** (1989) 837–862.
- [40] Zmitrowicz, A. An equation of anisotropic friction with sliding path curvature effects. *International Journal of Solids and Structures.* **36** (1999) 2825–2848.
- [41] Zmitrowicz, A. Illustrative examples of anisotropic friction with sliding path curvature effects. *International Journal of Solids and Structures.* **36** (1999) 2849–2863.
- [42] Zhang, H. W., He, S. Y., Li, X.S., Wriggers, P. A new algorithm for the numerical solution of 3D elastoplastic contact problems with orthotropic friction law. *Computational Mechanics.* **34** (2004) 1–14.
- [43] Zheng, Q.-S. Theory of representation for tensor function – A unified invariant approach to constitutive equations. *Applied Mechanics Reviews, ASME International.* **47** (1994) 545–587.

Contents

1	Introduction	1
2	Basis of the covariant description	3
2.1	Convective velocities. Variation of relative displacements.	4
2.2	Evolution equations for contact tractions	5
2.2.1	Integration of evolution equations. Geometrical interpretation of the return-mapping scheme.	5
2.3	Weak form.	6
3	Generalization for complex contact interface laws	6
3.1	Vector form of the isotropic equations	7
3.1.1	Elastic part of the contact deformation	7
3.1.2	Yield function for the isotropic Coulomb friction law	7
3.2	General interface model	8
3.2.1	Anisotropic evolution equations. Rate-independent model.	8
3.3	Anisotropic yield function	9
3.3.1	Various approaches for formulations of yield criteria and sliding rules . .	9
3.3.2	Coulomb type yield functions	10
3.4	Tensor representations for anisotropy	10
3.4.1	Spectral representation of the tensor – constant orthotropy in the plane.	11
3.4.2	Structure of the anisotropic tensor inherited from an arbitrary surface curvilinear coordinate system	12
3.4.3	Anisotropic plane. Structure of the \mathbf{B}^C and \mathbf{B} tensors in Cartesian coor- dinates.	14
3.4.4	Orthotropic surface in polar coordinates. Structure of the \mathbf{B}^C and \mathbf{B} tensors in Cartesian coordinates.	14
3.4.5	Spiral orthotropy on a cylindrical surface. Structure of the \mathbf{B}^C and \mathbf{B} tensors in cylindrical coordinates.	15
4	Derivation of the frictional contact problem via the principle of maximum dissipation.	17
4.1	Continuous formulation	18
4.2	Incremental formulation	19
4.2.1	Derivation of the sliding force \mathbf{T}^{sl}	21
4.3	Specification of initial conditions for the return-mapping scheme.	22
4.4	Derivation of the sliding incremental displacement $\Delta \boldsymbol{\xi}^{sl}$ and update scheme for the history variables.	22
4.5	Computational aspects for further implementation considering nonlinear and constant tensors.	23
4.5.1	A case with nonlinear tensors for large displacement problems	23
4.5.2	A case with constant orthotropy	23
4.6	Geometrical interpretation of the solution process.	24
5	Conclusion	27